High-Pressure Testing of Heterogeneous Charge Transfer in a Room-Temperature Ionic Liquid: Evidence for Solvent Dynamic Control

Tina D. Dolidze,[†,‡,§] Dimitri E. Khoshtariya,*[,†,‡,§] Peter Illner,[†] Leszek Kulisiewicz,[⊥] Antonio Delgado,[⊥] and Rudi van Eldik*[,†]

Inorganic Chemistry, Department of Chemistry and Pharmacy, University of Erlangen-Nürnberg, Egerlandstrasse 1, 91058 Erlangen, Germany, Institute of Molecular Biology and Biophysics, Gotua 12, 0160 Tbilisi, Georgia, Institute of Inorganic Chemistry and Electrochemistry, Mindeli 11, 0186 Tbilisi, Georgia, and Institute of Fluid Mechanics, University of Erlangen-Nürnberg, Cauerstrasse 4, 91058 Erlangen, Germany

Received: September 26, 2007; In Final Form: November 20, 2007

We report the first application of a high-pressure electrochemical strategy to study heterogeneous charge transfer (CT) in a room-temperature ionic liquid, [BMIM][BTA]. High-pressure kinetic studies on electron exchange for two redox couples of different charge type, viz. $[Fe(bipy)_3]^{3+/2+}$ and $[Fe(cp)_2]^{+/0}$, at bare Au electrodes within the range of 0.1−150 MPa, revealed large positive volumes of activation that were found to be virtually the same for the two redox couples in terms of the CT rate constants and diffusion coefficients, despite the reactant's charge type. Independent viscosity (fluidity) studies at elevated pressure (up to 175 MPa), were also performed and revealed a pressure coefficient closely resembling the former ones. Complementary temperature-dependent kinetic studies within the range of 298−358 K also revealed the virtual similarity in activation enthalpies for the same kinetic and diffusion processes, as well as the viscosity of [BMIM][BTA]. A rigorous analysis of the complete variety of obtained results strongly indicates that dynamic (frictional) control of CT is operative by way of the full adiabatic mechanism. The contribution of the Franck−Condon term to the activation free energy of the kinetic process seems almost diminished because of the high value of electronic coupling and freezing out of the outer-sphere reorganization energy. Further analyses indicate that frictional control most probably takes place through slow translational modes (implying "minimal volume" cooperative dislocations) of constituent ions. This kind of motion seems further slowed down within the vicinity of the active site presumably located within the diffusive-like zone situated next to the compact (first) part of the metal/ionic liquid junction.

1. Introduction

Outer-sphere electron transfer (ET) processes in irregular condensed-phase media are of current importance for biological and technological applications. Despite great efforts in this direction, we are only at the beginning of a rigorous understanding of ET intrinsic mechanisms. Electrochemical approaches are among the most effective and successful tools for this purpose, thanks to the availability of a variety of convenient methodological resources including all instrumental, preparative, and theoretical aspects.[1] Importantly, by working with electrochemical and bioelectrochemical systems, one is able (but not restricted) to deal with a single redox-active component, with an electrode acting as another reactant, a circumstance that simplifies, when required, experimental and theoretical handling. Furthermore, the ability to systematically and gradually vary intrinsic ET parameters should be mentioned.[1,2] Among the disadvantages of electrochemical approaches, in the case of molecular liquids used as solvents, the conventional need to add a considerable amount of the supporting electrolyte necessary to provide sufficient conductivity should be mentioned (*vide infra*).[1] In terms of a microscopic description of ET (implying a single inherent barrier-crossing event), for a variety of electrochemical and bio-electrochemical systems, two specific mechanistic patterns have been identified (both theoretically and experimentally), corresponding to long-range and short-range ET motifs. In the case of short-range ET involving either bare electrodes (in most cases, made of Au, Pt, Ag, or Hg), or when these are modified by thin films (<10 Å), the adiabatic mechanism is operative, which implies solvent dynamic (frictional) control of ET, *vide infra*.[2b−d] In contrast, in the case of thick (>10 Å) insulating spacers (most commonly, self-assembled monolayer films (SAMs)), the non-adiabatic (long-range tunneling) regime is encountered.[2]

In a "classical" case where the pre-equilibrium step is not accompanied by the notable adsorption of reactant species on the electrode surface (freely diffusing regime), and the charge-transfer (CT) step by considerable inner-sphere reorganization,[1,2] the experimental standard heterogeneous rate constant can be presented as a product of two components (eq 1):[3]

$$k^0_{EXP} = k^0_{ET} K_A = k^0_{ET} \delta R_e \exp\left(\frac{-\Delta G_A}{RT}\right) \qquad (1)$$

where K_A is the statistically averaged equilibrium constant proportional to the probability of finding the reactant species at the reactive site near the electrode, usually considered as the outer Helmholtz plane (OHP), δR_e is the "effective thickness" of the planar reaction zone (which is expected to have a value

* Corresponding authors. E-mail: dimitri.k@joker.ge(D.E.K.); vaneldik@chemie.uni-erlangen.de (R.v.E.).
† Inorganic Chemistry, University of Erlangen-Nürnberg.
‡ Institute of Molecular Biology and Biophysics.
§ Institute of Inorganic Chemistry and Electrochemistry.
⊥ Institute of Fluid Mechanics, University of Erlangen-Nürnberg.

10.1021/jp077734j CCC: $40.75
Published on Web 02/16/2008

on the order of 2×10^{-9} to 10^{-8} cm^3), reflecting the major portion of the space integral over the intrinsic CT constant (k^0_{ET}), ΔG_A is the equilibrium free energy required to bring the reactant ion to the active site near the electrode (presumably to the OHP), R is the gas constant, and T is the absolute temperature.

In the intrinsic regime of strong electronic coupling (typical for short-range ET; see Results and Discussion for details), when the adiabatic (solvent control) mechanism is operative, the updated expression for k^0_{ET} reads as eq 2[4] (however, see refs 5 and 6 for variations):

$$k^0_{ET} = \nu_{eff}\left(\frac{\lambda}{\pi^3 RT}\right)^{1/2} \exp\left(\frac{-\Delta G^*_{ET}}{RT}\right) \quad (2)$$

where ν_{eff} is a characteristic frequency for the relaxation of solvent molecules coupled to ET, and λ and ΔG^*_{ET} are the reorganization and activation free energy parameters, respectively. Whatever medium relaxation is involved, it is essentially related to the solution viscosity (or to the local viscosity, in some special cases such as a biological environment[2c,d]). Hence, the general experimental signature of solvent dynamic control (adiabaticity) of intrinsic ET is the relation (eq 3)

$$k^0_{ET} \propto \eta^{-\delta} \quad (3)$$

where, in the uncomplicated case of the full adiabatic regime, $\delta = 1$ (in general, $0 \leq \delta < 1$, where the value of δ reflects either the degree of adiabaticity or the degree of dynamic coupling of the redox center's immediate environment with the area where the medium's viscosity can be directly varied[2b−d]). Hence, the key methodological tool for a verification or rejection of the solvent friction mechanism is a change in the solution dynamic properties that can be achieved through the variation of the solvent (reaction medium) as such,[1b,5−7] by the addition of viscous additives to a given solvent[2b,d,7,8] or through the direct altering of the medium dynamic properties by the variation of temperature[1a,b,9,10a] or pressure.[1c,9b,10,11] Each of these approaches have advantages and disadvantages. However, in uncomplicated cases, all these unambiguously pointed to the solvent control mechanism for outer-sphere electrochemical ET at bare metal electrodes,[2b,d,6−8,10] and, in few studied cases, at thin SAMs.[2b−d,9c,11]

Perhaps the strategy of pressure variation is the most straightforward because it allows the effective change of the solution dynamic characteristics without changing their chemical composition.[1c,10−12] Also, the disadvantageous complications due to the double-layer effects that accompany electrochemical methodologies probably show up to a lesser extent in electrochemical high-pressure kinetic experiments as compared to analogous temperature-dependent studies[1c,10a] (*vide infra*). Indeed, high-pressure electrochemical kinetic studies were shown to be strikingly effective in the context of studies of outer-sphere ET mechanisms occurring in organic molecular liquids[1c,10] and in the interior of the model redox protein cytochrome *c*.[2c,d,11] Specifically, it has been unequivocally demonstrated that the frictional control by the reactant environment (characterized by its local viscosity) shows up through a notable decrease in the ET rate constant, hence resulting in a positive volume of activation (*vide infra*).[1c,9b,10,11] As an exception, friction control cannot be disclosed by pressure variation in processes with water as an immediate environment in experiments performed around room temperature (20−25 °C), due to unique features of water,[1c,10b] but can be rather effective for ET in organic solvents or involving proteins dissolved in aqueous solution, since the protein interior, at least in part, behaves like any other nonaqueous medium.[2c,d,11]

The volume of activation for the intrinsic CT stage can be presented by eq 4:[1c,9b,10−13]

$$\left[\frac{\partial(\ln k^0_{ET})}{\partial P}\right]_T = -\frac{\Delta V^*_{ET}}{RT} \quad (4)$$

For the case of freely diffusing redox species, the heterogeneous standard rate constant, k^0_{EXP}, rather than the intrinsic standard rate constant, k^0_{ET}, can be determined through the electrochemical experiment to yield ΔV^*_{EXP} instead of ΔV^*_{ET}. Furthermore, it has been demonstrated[10a] that pressure effects on the pre-equilibrium constant, K_A, are of minor importance within the range up to 200 MPa, resulting in a negligible value for the corresponding volume contribution ($\Delta V_A \approx 0$) and, hence, $\Delta V^*_{EXP} \approx \Delta V^*_{ET}$. Moreover, for the model electrode ET process involving $[Fe(Me_5cp)_2]^{+/0}$ (Me = methyl, cp = cyclopentadienyl), which proceeds in a series of organic molecular solvents, it has been demonstrated that $\Delta V^*_{EXP} \approx \Delta V^*_{ET} \approx \Delta V^*_{Flu} \approx \Delta V^*_{Diff}$, where ΔV^*_{Flu} is the activation volume of the solvent fluidity (reciprocal viscosity), and ΔV^*_{Diff} is the activation volume for diffusion of the reactants. This result has been convincingly interpreted in terms of the dynamic control mechanism for heterogeneous ET (*vide infra*).[1c,10]

Analogously, for the effect of temperature on k^0_{ET}, the enthalpy of activation can be written as in eq 5 (which, under certain conditions, yields Arrhenius-like quasi-linear plots, *vide infra*; see. e.g., ref 13):

$$\left[\frac{\partial(\ln k^0_{ET})}{\partial(1/T)}\right]_P = -\frac{\Delta H^*_{ET}}{R} \quad (5)$$

Unfortunately, the situation with this issue is not so straightforward as with variable pressure studies, probably because the contributions of the free energy components (ΔH_A and ΔS_A) to the exponential term of eq 1, unlike the component ΔV_A, are not negligible because of the highly complex (multisheet) structure of the interfacial double-layer zone in (or near) which the redox-active reactant species are to be situated in due course of the electron exchange. A strong indication of this effect, which can show up as additional enthalpy or entropy contributions (ΔH_A and ΔS_A) to ΔG^*_{EXP}, comes from recent data of Matsumoto and Swaddle,[10a] who found that the value of ΔH^*_{EXP} for the same redox couple and solvent may significantly vary with the supporting electrolyte concentration (see Results and Discussion). Hence, the corresponding results for the activation enthalpy and entropy should be considered with caution. Equations analogous to eqs 4 and 5 can be applied to diffusion coefficients to yield the values of ΔV^*_{Diff} and ΔH^*_{Diff}, which, in direct comparison with ΔV^*_{ET} and ΔH^*_{ET}, seems to be useful (*vide infra*).

As mentioned above, despite great progress in studies of electrochemical ET mechanisms, the present understanding is far from complete and requires additional efforts. It is commonly accepted that, in the solvent control (adiabatic) regime (eq 2), the Debye-type reorientational relaxations are the microscopic events that determine the solvent frictional control over ET via the parameter ν_{eff}.[1c,2b,6−8,10,11] Zusman[18] theoretically considered the role and possible contribution of the "polarization diffusion" of pure dipolar liquids to the parameter ν_{eff} (and, hence, to the corresponding rate constant, k^0_{ET}, eq 2), and came to the conclusion that it can be significant for adiabatic processes in certain organic liquids (*vide infra*). Marcus[19] gave a classifica-

tion of different ionic capacities in various ET processes, however, skipping solvent control through ion relaxation. Buttry and Anson[20] and Murray et al.[21] considered ionic motion (diffusion) as a main controlling event for homogeneous and heterogeneous ET by a mechanism that differs from the intrinsic adiabatic pattern mentioned above. A new and promising extension of earlier electrochemical and homogeneous CT mechanistic studies performed in aqueous solutions and organic molecular liquids is connected with the application of *room-temperature ionic liquids (RTILs*) as solvents. This relatively new type of solvent displays unique properties that were proven to be advantageous for various technological purposes, as well as for novel fundamental investigations.[14,15] Regarding electrochemical assemblies, it is essential that exploitation of these liquids (the constituent components of which carry single net charge and provide sufficient conductivity) simplifies the overall solution composition and avoids the addition of extra (electrolyte) constituents.[15] The latter normally adsorb, or are active at the electrode/solution interface, in (or near) which the reactant particles are situated.[1] Indeed, recent experimental and theoretical work indicated a rather tractable double-layer structure for the representative RTILs[16] compared to the case of most typical conventional (molecular) liquids.[1,2] Therefore, application of RTILs may shed new light on the fundamental problem of the nature of a mode-controlling relaxation process in the CT solvent friction (adiabatic) mechanism.

Several studies on rate processes, both homogeneous[22] and heterogeneous,[15] that proceed in RTILs have been reported. Among them, a sequence of specific advantages of these solvents for electrochemical investigations have been underlined.[15] Our reasoning additionally indicated that (a) the application of kinetic electrochemical methodology (especially when coupled with the high-pressure technique[1c,2c,d,9b,10−12]) unequivocally identifies the true ET event, whatever solvent (molecular or ionic) is employed and whatever intrinsic mechanism is operative; (b) RTILs seem to be convenient solvents for electrochemical studies because, at least, they do not require extra additives to maintain sufficient ionic conductivity,[26] and are also considered to form reasonably interpretable double layers (see ref 16); (c) because of these reasons, RTILs may serve as excellent media for fundamental studies of intrinsic ET mechanisms, especially those microscopic aspects that are connected with the identification of the relaxation process(es) "frictionally" controlling ET in the adiabatic regime.

For the latter purpose, we combined in the present study electrochemical methodology with the strategy of high-pressure kinetic studies that is ideally suitable for a variation of the solvent dynamic characteristics such as the variety of relaxation times, diffusion coefficients, and so forth, without changing the solvent's chemical composition. We report here high-pressure (up to 150 MPa) kinetic studies of the CT intrinsic mechanism in a typical, well-studied RTIL, [BMIM][BTA], for two representative redox couples—$[Fe(bipy)_3]^{3+/2+}$ and $[Fe(cp)_2]^{+/0}$ (bipy = bipyridine, and cp = cyclopentadienyl)—displaying rather different charged states and formal redox potentials (*vide infra*). These circumstances are important for profound understanding of potentially significant double-layer effects through the comparative analysis of the behavior of respective heterogeneous standard rate constants of CT. The systematic measurements of these parameters along with the reactant diffusion coefficients and formal (equilibrium) redox potentials (vs the Ag wire electrode) were performed employing cyclic voltammetric (CV) methodology with the fast-scan extension.[1a,24] For comparison, complementary temperature studies (20−85 °C) have also been performed, and the respective results are discussed in a combined manner. In addition, the equilibrium electrostriction effects were deduced from the accompanying equilibrium measurements and compared with similar results available for molecular liquids.

2. Experimental Section

A. Materials. The RTIL 1-butyl-3-methylimidazolium bis(trifluoromethylsulfonyl)imide, [BMIM][BTA], was synthesized and purified according to known procedures[22a,b] and kept under nitrogen atmosphere. The water content of this ionic liquid was determined by the Karl Fischer titration procedure using a Metrohm 765 KF Coulomb meter and found to be 55 ± 6 ppm.

Dicyclopentadienyliron (ferrocene), $[Fe(cp)_2]^0$ (98%) and tris(2,2-bipyridine)iron(II) hexafluoro phosphate complexes were obtained from Sigma-Aldrich and used as received. All solutions were prepared under a nitrogen atmosphere.

B. Electrochemical Measurements and Data Processing. The pressure vessel and electrochemical cell were described in detail before.[2d,11] The working electrode was a 1.6 mm Ø gold disc electrode sealed in a Teflon cylinder (BAS). The working electrode, together with the auxiliary electrode (platinum wire) and quasi-reference electrode (silver wire, placed in a plastic tube with a Vycor tip at the end) were sealed into the cell cap by two O-rings. The working volume of the high-pressure electrochemical cell was 5 mL. The assembled pressure vessel containing the cell was placed in a thermostated water jacket equilibrated at the desired temperature. The temperature was controlled within ± 0.1 °C using a digital temperature controller. Working solutions were purged with nitrogen for at least 15 min before experiments, and the nitrogen stream was kept over the solution during the experiments (however, not for the high-pressure cell). The variable pressure measurements were performed with pressure steps of 25 MPa starting at $P = 5$ MPa (to eliminate any small bubbles) and after each cycle pressure was lowered to the same value for checking the measurements. Care was taken that the results obtained at the start and end of the pressure cycle were in good agreement.

Under ambient pressure conditions, electrochemical measurements at different temperatures were performed in a three-electrode cell equipped with a water jacket. The gold (1.6 mm diameter, BAS) and glassy carbon (3 mm diameter, Metrohm) disk electrodes were used as working electrodes, together with a large platinum wire auxiliary electrode. The quasi-reference electrode used was a silver wire, placed in a plastic tube with a Vycor tip at the end. This kind of reference electrode is conventionally used, especially within the field of ionic liquid electrochemistry (see the review article in ref 15a). The stability and reproducibility of this quasi-reference electrode was sufficient to determine the temperature-induced midpoint potential gradual shift of ca. 0.15 V with high accuracy (see Figure 14 below).

The working electrodes were cleaned before each pressure/temperature cycle by polishing with alumina slurry (0.3 and 0.05 μm alumina powder) on a Buehler polishing pad washed with Millipore water followed by sonification. Finally, electrodes were rinsed with ethanol and dried in a nitrogen stream. In the case of ferrocene as reactant when the Au electrode was used, a slight slowing down of the reaction rate was observed over time, especially at high temperatures, obviously due to passivation of the electrode surface.[9b,23] To exclude the above-mentioned effect on the temperature dependence of the measured rate constant in the case of ferrocene, the following procedures were applied: (a) the electrode surface was cleaned before each

TABLE 1: The Midpoint Potentials (vs Ag Wire), Heterogeneous Standard Rate Constants and Diffusion Coefficients for the $[Fe(bipy)_3]^{3+/2+}$ and $[Fe(cp)_2]^{+/0}$ Redox Couples under "Normal" Conditions[a,b]

		$P_o = 5$ MPa[c], $T_o = 20$ °C[c]		$P_o = 0.1$ MPa[d], $T_o = 25$ °C[d]	
redox couple	E^0, V[d]	k^0_{EXP}, cm s^{-1}	D_R, cm^2 s^{-1}	k^0_{EXP}, cm s^{-1}	D_R, cm^2 s^{-1}
$[Fe(bipy)_3]^{3+/2+}$	0.986	3.0×10^{-3}	5.0×10^{-8}	3.6×10^{-3}	7.5×10^{-8}
$[Fe(cp)_2]^{+/0}$	0.290	4.9×10^{-3}	2.2×10^{-7}	5.3×10^{-3} (6.0×10^{-3})[e]	2.9×10^{-7}

[a] Start settings for the pressure and temperature cycles were somewhat different because of the different methodological designs. [b] The average error for experimental kinetic parameters is estimated to be within 10%. [c] Start setting for pressure-dependent kinetic studies. [d] Start setting for temperature-dependent kinetic studies. [e] Value obtained using the computer CV fitting procedure (see Experimental Section and Figure 3).

temperature measurement; (b) for comparison purposes, the temperature measurements were also performed using a glassy carbon electrode. In the case of the high-pressure studies, duration of experiments was minimized as much as possible, and numerous control experiments at different reagent concentrations were performed.

Electrochemical measurements were carried out with an Autolab Electrochemical Analyzer PGSTAT 30, equipped with the General Purpose Electrochemical System (GPES) software for Windows (version 4.9). Autolab software was used for a variety of data analyses, including CV curve fitting and the "post-measurement" Ohmic potential drop (*IRe*) corrections (*vide infra*).[1a] Conventional fast scan CV[1a] was used throughout this work. It allows very accurate and prompt calculation of rate constants for simple (uncomplicated) ET reactions by changing the potential scan rate to set conditions where the reaction exhibits kinetic behavior, indicated by increased separation of the cathodic and anodic peak potentials (ΔE_p) and to calculate the standard rate constant of ET (k^0_{EXP}) from the numerically evaluated relationship between (ΔE_p) and the Ψ function according to Nicholson[1a,24] using eq 6:

$$\Psi = \frac{(D_O/D_R)^{\alpha/2}\,(RT)^{1/2}\,k^0_{EXP}}{(\pi n F D_O \upsilon)^{1/2}} \qquad (6)$$

where α is the transfer coefficient, D_O and D_R are the diffusion coefficients of the oxidized and reduced forms, respectively, υ is the scan rate, and n is the number of transferred electrons. Values of diffusion coefficients were deduced from CV response at slow scan rates, and values of $\alpha \approx 0.5$ (for both redox couples) were gained from the fitting procedure. In this work, the full computer fitting procedure (*vide infra*) was applied in a few cases for illustrative purpose only, in order to demonstrate that the whole shape of the CV curve is consistent with the genuine ET event. In most cases, we applied the original method of Nicholson, which, in fact, is a simplified fitting procedure using two fixed key points. We found both procedures to yield similar results for rate constants (validating an average experimental error within 10%, Table 1; *vide infra*). The reported values of α (Table S1, Supporting Information) are digital values generated by computer as a result of the full computer fitting procedure. These values are also presented for illustrative purposes, to demonstrate the overall consistency (Table S1). We note that, within the Nicholson procedure, values of ΔE_p, in general, are *nearly* independent of α in the range $0.3 < \alpha < 0.7$.[24a] However, our fitting procedure always yielded the values of $\alpha = 0.50 \pm 0.05$, which can be interpreted as a further indication of an almost ideal symmetric shape of our experimental CV curves. Furthermore, one should keep in mind that the standard Nicholson method is based on the Butler−Volmer model for the relation between the ET rate and the electrode potential, which is a limiting case of the more general Marcus theory.[32a] However, in the case of relatively small peak-to-peak separations, i.e., when the reaction free energy is substantially less than the Marcus reorganizational free energy, λ, i.e., when $\Delta E_p/2 \ll \lambda$, both the models give similar results. However, one should not confuse the role of the Marcus theory regarding the electrochemical methodology (allowing for some simplifications under certain conditions; present section) with its fundamental application (see Results and Discussion below).

We have readily extended the Nicholson's "two point" (Ψ vs ΔE_p) algorithm to temperatures different from 25 °C[25] by using "analytical" eq 7 derived for this particular temperature.[1c]

$$\ln \Psi = 3.69 - 1.16 \ln(\Delta E_p - 59) \qquad (7)$$

These relationships at temperatures of our present interest (except 25 °C) have not been published so far (see, however, ref 25b). The values of Ψ as a function of ΔE_p for temperatures that are relevant to this work are presented in Figure S1 (see Supporting Information).

Typical CVs recorded at low scan rates under different pressure and temperature conditions are presented in Figure 1. All the CVs were free of pre- and post-peaks. The differences between peak (E_p) and half peak ($E_{p/2}$) potentials at scan rates up to 0.5−1 V s^{-1} at all temperatures and pressures are in good agreement with corresponding theoretical values (for example, $(E_p - E_{p/2}) \approx 58$ mV at 25 °C and ≈ 70 mV at 85 °C) according to eq 8:[24b]

$$E_p - E_{p/2} = 2.22RT/nF \qquad (8)$$

Peak-to-peak separation at low scan rates (up to 0.5 V s^{-1}) at 20 °C within the pressure range (0−150 MPa) was 66−67 mV and not significantly dependent on pressure. ΔE_p within the temperature range of 25−85 °C (at $P = 0.1$ MPa) was 64−80 mV. In all cases, the plot of background-corrected peak current ($I_{p(corr)}$) as a function of the square root of the scan rate, $\upsilon^{1/2}$, is linear and passes through the origin (Figure 2), indicating that the ET reaction is not complicated by accompanying adsorption and/or chemical processes. Experimental CVs at low scan rates fit well to the reversible uncomplicated single ET process. Hence, all the above-mentioned facts indicate that, at low scan rates throughout all the pressure- and temperature-dependent experiments, recorded CVs exhibit reversible behavior (reactions are diffusion controlled). The diffusion coefficients for reduced (initial) forms of reactant ions, D_R, were calculated from the slope of the dependence of $I_{p(corr)}$ on $\upsilon^{1/2}$ using eq 9:[1a]

$$I_{p(corr)} = -0.446nF\left(\frac{nF}{RT}\right)^{1/2} C_o D^{1/2} \upsilon^{1/2} \qquad (9)$$

Because the ratio for $I_{p(Red)}$ and $I_{p(Ox)}$ was always close to unity, for simplicity reasons we assumed that $D_R \approx D_O \approx D$. This assumption introduced minor errors in the subsequent calculations using eq 6. The average experimental error for the determination of D estimated from two to four independent

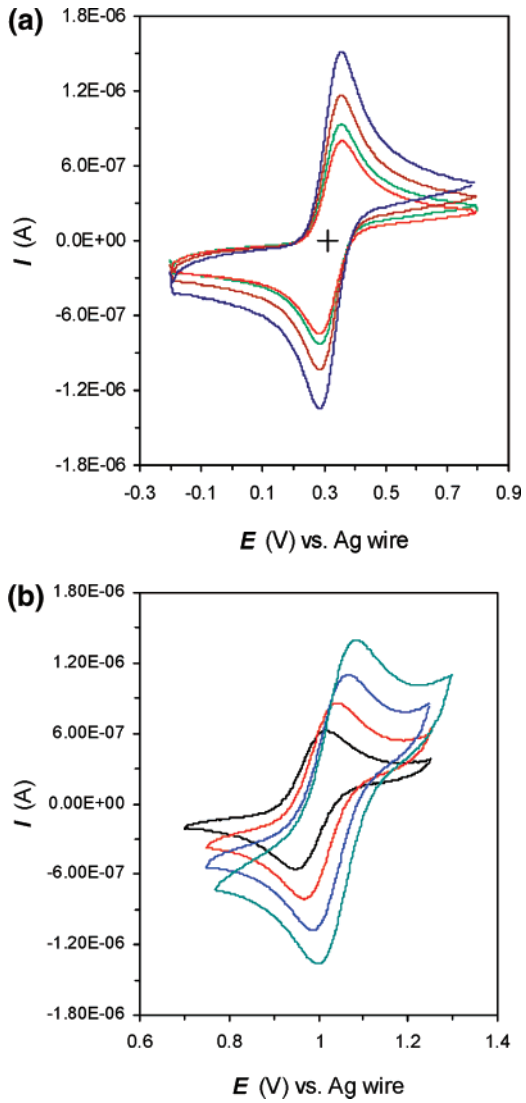

Figure 1. (a) CVs for the $[Fe(cp)_2]^{+/0}$ couple (2.4×10^{-3} M) recorded with the Au electrode at different pressures: $P = 5$, 50, 100, and 150 MPa (peak current decrease), $T = 20$ °C, $\upsilon = 0.05$ V s^{-1}. (b) CVs for the $[Fe(bipy)_3]^{3+/2+}$ couple (2×10^{-3} M) recorded with the Au electrode at different temperatures: $T = 25$, 45, 65, and 85 °C (peak current increase), $P = 0.1$ MPa.

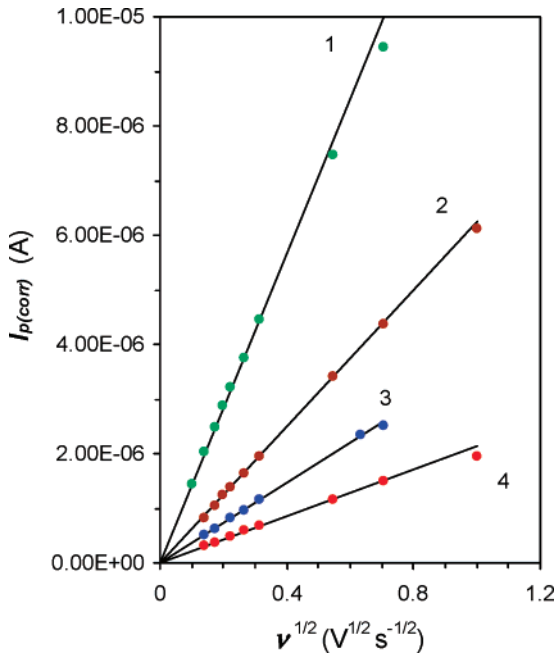

Figure 2. Dependence of the background corrected anodic peak current on the square root of the scan rate obtained for different concentrations of $[Fe(cp)_2]^{+/0}$ (1) and $[Fe(bipy)_3]^{3+/2+}$ (2−4) with the Au electrode under the following pressure and temperature conditions: (1) $T = 25$ °C, $P = 0.1$ MPa, $c = 5 \times 10^{-3}$ M; (2) $T = 85$ °C, $P = 0.1$ MPa, $c = 2 \times 10^{-3}$ M; (3) $T = 20$ °C, $P = 50$ MPa, $c = 3 \times 10^{-3}$ M; (4) $T = 20$ °C, $P = 100$ MPa, $c = 3 \times 10^{-3}$ M.

experiments in most cases was within 10% (for standard cases, it was within 5%, and in a few other cases, within 14%). The actual error bars in Figures 6, 8, and 9 (not shown for brevity) are 2 times larger than the selected figure symbols. At high scan rates, peak-to-peak separation increased (see Figure S2a,b, Supporting Information) and values of standard rate constants at different pressures and temperatures could be calculated by the method of Nicholson,[1a,24] eq 6 (for some illustrative examples, see Tables S1−S3, Supporting Information). In the ionic liquid case, the diffusion coefficients are small enough for the reversibility to be approached with rather slow rate constants. The rate constants are considerably slower than those for the same redox couples dissolved in organic solvents because of the solvent dynamic control mechanism that operates at much higher viscosity of the medium (*vide infra*). However, this was a great advantage in our studies because the scan rates up to 10 V/s were sufficient to attain a ΔE_p on the order of 70−100 mV, allowing determination of rate constants with a sufficiently high accuracy. Indeed, although the reproducibility of absolute values for rate constants over independent series of experiments varied within 20−30%, including series with similar or alternative experimental conditions (variation of reactant concentrations, electrode type or surface area, etc.), the average experimental error for relative values estimated from two to four different series was, in most cases, with a few exceptions, within 10% (±5%). Importantly, the control points taken at the end of each pressure and temperature cycle all fall within the same range of experimental uncertainty. The relative values of rate constants plotted in Figures 5, 7, and 10 changed approximately four to five times upon pressure or temperature variation within the indicated ranges. At the same time, the actual error bars in Figures 5, 7, and 10 (not shown) are only twice as large as the depicted figure legends.

C. Approval of the Genuine CT Pattern. To further prove that measured rates strictly reflect genuine ET rates, the fitting procedure of experimental CVs obtained at high scan rates with theoretical quasi-reversible CVs have been performed (Figure 3), allowing the evaluation (calculation) of electrochemical standard rate constants of ET (k_{el}^0) from the value of the normalized current (k) gained from the fitting procedure through eq 10 using GPES Software (recall, however, the above-mentioned restrictions when using the formulas based on the Butler−Volmer model):

$$k = k_{el}^0 (RT/nF\upsilon D)^{1/2} \qquad (10)$$

Values of standard rate constants gained from the fitting procedures are in excellent agreement with calculated values, indicating that the measured k_{el}^0 values correspond to the actual ET rates. Values of k_{el}^0 and ET coefficient α for ferrocene obtained from the fitting procedure along with the corresponding experimental values are presented in Table S1.

D. Correction for the Ohmic Drop. CV response in RTILs (due to the high viscosity of these solutions, especially at high scan rates) can be distorted (the effect of Ohmic polarization), causing notable enhancement of the peak-to-peak separation and,

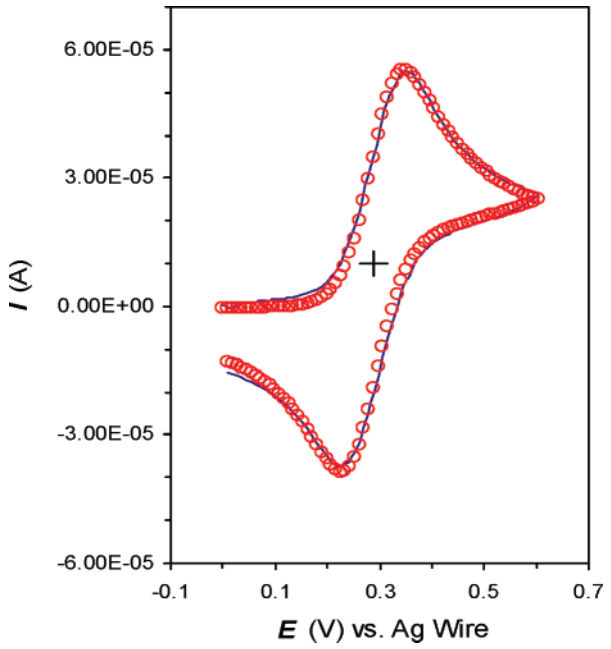

Figure 3. Experimental CV of $[Fe(cp)_2]^{+/0}$ (5×10^{-3} M) recorded with the Au electrode at $P = 0.1$ MPa, $T = 65$ °C, and $v = 4$ V s^{-1} (calculated value of $k^0_{EXP} = 8.1 \times 10^{-3}$ cm s^{-1} using eq 6) along with the fitted quasi-reversible one-electron transfer model (circles); results obtained from the fitting procedure: $k^0_{Fitt} = 9 \times 10^{-3}$ cm s^{-1}; transfer coefficient $\alpha = 0.5$ (see Experimental Section for further comments).

consequently, giving lower values of the rate constant (k^0_{el}). However, the corresponding corrections were found to be negligible when a reactant concentration as low as 5×10^{-4} M was used. The rate constants determined at these concentrations were similar to those determined at higher concentrations with the application of the post measurement *IRe* drop correction[1a] adopted in this work (*vide infra*). Anyway, unlike the absolute values of the rate constants, the dependence of k^0_{el} on pressure and temperature measured in this work is free of the relative influence of Ohmic drop because an increase/decrease in resistance (*Re*) with increasing pressure or temperature causes a corresponding decrease/increase in current (*I*). These two values cancel each other with respect to the *IRe* term.[2b,7a,11a,26] As evidence for this cancellation, dependences of the uncorrected *IRe* term values of k^0_{el} on pressure and temperature measured at different concentrations of reactant and/or different scan rates (actually the case where values of *I* are different) have the same slope. Moreover, although the values of rate constants calculated from the post measurement *IRe* drop-corrected CVs are higher than the corresponding uncorrected values, they show the same dependence on pressure and temperature (e.g., see Figure S3 and Table S2, Supporting Information).

The solution resistance *Re* between the surface of the working electrode and the tip of the reference electrode was calculated using eq 11:[27]

$$Re = \arctan\left[(r_r/r_w)/2\pi\, r_w \kappa\right] \qquad (11)$$

where r_w is the radius of the working electrode (in the present case, 0.08 mm), κ is the conductivity of the medium (3.9 S m^{-1} at 20 °C[15a]), and r_r is the distance between the working and reference electrodes, which was positioned 1.0 cm from the working electrode. As one can see from eq 11, resistance of the solution is mainly determined by the solution conductivity and the electrode area. The calculated value of *Re* was 760 Ω at 20 °C. As an illustration, the values of *Re* at temperatures other than this were calculated taking into account changes in conductivity/viscosity with temperature (see Table S2).[22b] However, as mentioned above, by handling the alternative series of experiments with reactant concentrations as low as 5×10^{-4} M, we were able to minimize the Ohmic drop corrections and even make them negligible.

Furthermore, within the context of remarkable chronicles regarding electrochemical kinetic studies of the ferrocene redox couple in molecular liquids such as acetonitrile (thoroughly reviewed in ref 6d), one may question whether the deduced rate constant as low as 5.3×10^{-3} cm s^{-1} (under standard conditions, Table 1), despite the arguments presented above, is physically justified. The "best values" of rate constants on the order of 1 cm s^{-1} (or slightly higher) have been established for a typical model system ($[Fe(cp)_2]^{+/0}$ in acetonitrile, 0.5 M TBAP, Pt electrode) compared to "rejected" values of 0.01−0.1 cm s^{-1} on the one hand, and 220 cm s^{-1} (!) on the other.[6d] As it will be shown in the next section, our present value of 5.3×10^{-3} cm s^{-1} is essentially related to the solvent viscosity due to the dynamical control regime. Seemingly, the same regime holds in the case of acetonitrile solutions (see refs 10a and 10e). Provided the exponential terms in eq 2 are of the same or comparable value, at least a 130-fold difference in rate constants (of total 200 to 300-fold) can be readily attributed to the large difference in solution viscosities (44.7 cp for [BMIM][BTA] vs 0.34 cp for acetonitrile at 25 °C). The remaining minor (1.5 to 2.5-fold) difference in rate constants can be accounted for by the difference in the impact of double-layer structures (i.e., the term K_A in eq 1), which does not seem surprising taking into account the variance between the interfacial ion−molecular assemblages under comparison.

E. Density and Viscosity Measurements as a Function of Pressure. The dynamic viscosity was determined as a function of pressure with a high-pressure rolling ball viscosimeter via the measurement of time *t* that a steel sphere needs to move along a defined distance inside an inclined tube filled with the solvent. The rolling time *t* was measured by an inductive method using a time counter triggered by pick-up coils mounted on the measurement tube. The dynamic viscosity η was then calculated according to eq 12:

$$\eta = Pt(\rho_s - \rho) \qquad (12)$$

where *P* is a pressure and temperature-dependent calibration factor, ρ_s is the density of the steel sphere, and ρ is the density of the sample at a specific pressure. The pressure inside the measurement tube was generated by a manual piston pump. Temperature control was provided by a glycol jacket connected to a thermostat. The viscosimeter was filled with the investigated ionic liquid in a controlled nitrogen atmosphere in order to protect the sample from contact with air humidity. Since the applied rolling ball viscosimeter provides relative data, viscosity measurements under ambient conditions were necessary for the purpose of calibration. The required measurements were carried out with a dynamic stress rheometer Paar Physica UDS 200 (Anton Paar, Germany). A detailed description of the applied measurement setup and experimental procedure can be found in the literature.[28a,b]

The density/compressibility of the ionic liquid as a function of pressure was measured with a screw press to reach the required pressure. The press was connected to a pressure sensor and the ionic liquid reservoir to fill it. There was also an

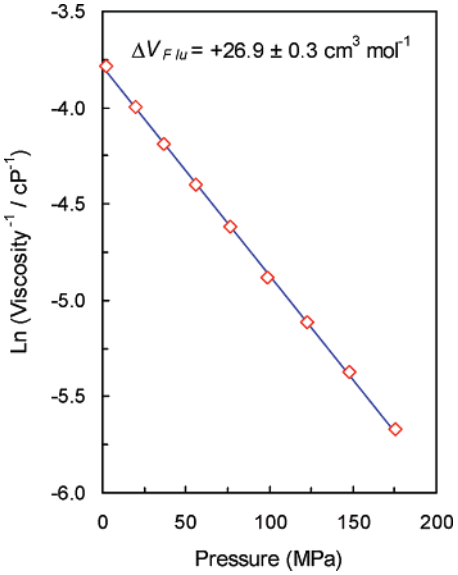

Figure 4. High-pressure effect on [BMIM][BTA] fluidity (reciprocal viscosity) from this work (see text for experimental details).

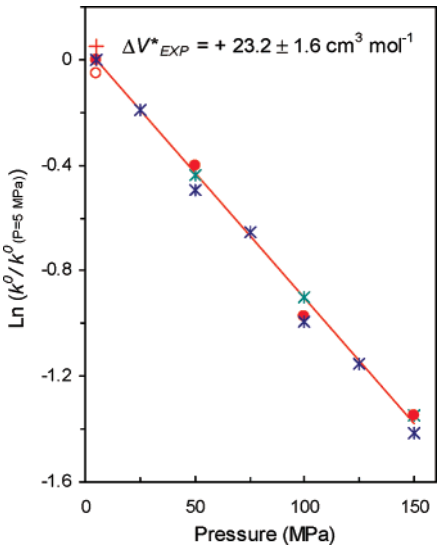

Figure 5. High-pressure effect on the rate constant for $[Fe(bipy)_3]^{3+/2+}$ (asterisks) and $[Fe(cp)_2]^{+/0}$ (circles) electron exchange at the Au electrode in the ionic liquid [BMIM][BTA] at 20 °C.

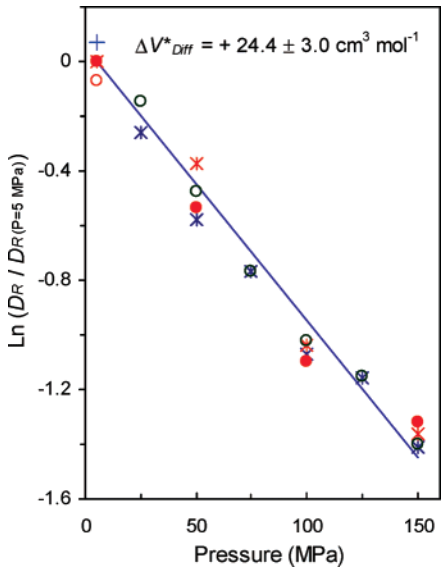

Figure 6. High-pressure effect on the diffusion coefficient for $[Fe(bipy)_3]^{3+/2+}$ (crosses/asterisks) and $[Fe(cp)_2]^{+/0}$ (circles) electron exchange at the Au electrode in the ionic liquid [BMIM][BTA] at 20 °C.

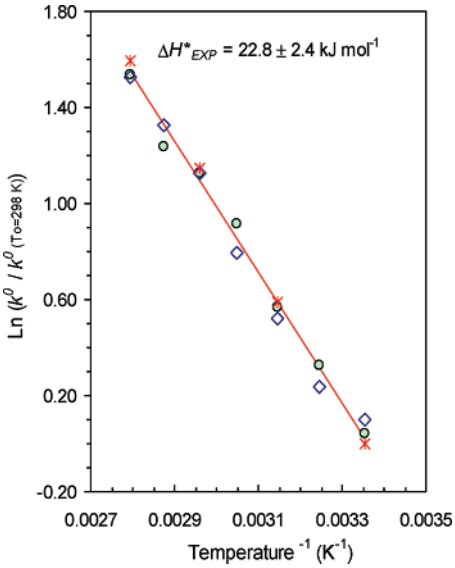

Figure 7. Temperature effect on the rate constant for $[Fe(bipy)_3]^{3+/2+}$ (circles) and $[Fe(cp)_2]^{+/0}$ (rhombs/asterisks) electron exchange at the Au electrode in the ionic liquid [BMIM][BTA] at ambient pressure.

additional valve in the pressure line for a quick release of pressure. The screw press had a specific volume of 15 mL, which could be reduced in steps of 0.1 mL. The compressibility of the tested ionic liquid was calculated by the quotient of the volume change divided by the whole liquid volume of the system and the change in pressure, viz. $\kappa = -\Delta V/V \times dP$. The resilience of the steel tubes could be disregarded because of the very low elasticity modulus of the used steel. A detailed description of the method can be found in the literature.[28c] Viscosity data as a function of pressure are collected in Table S4 (Supporting Information), and the logarithm of $1/\eta$ (fluidity) vs P is plotted in Figure 4.

3. Results and Discussion

A. Impact of Pressure and Temperature on Rate constants and Diffusion Coefficients. The values of *IRe*-corrected (experimental) heterogeneous standard rate constants of electron exchange at zero overvoltage, k^0_{EXP}, for $[Fe(bipy)_3]^{3+/2+}$ and $[Fe(cp)_2]^{+/0}$ at the bare Au electrode in [BMIM][BTA], along with the matching diffusion coefficients, D_R, under ambient conditions (standard states that differ somewhat for the pressure and temperature cycles) are presented in Table 1. The semi-logarithmic dependences of the heterogeneous standard rate constants, and diffusion coefficients (reduced to their standard values) on hydrostatic pressure are presented in Figures 5 and 6, respectively. The corresponding dependences on the reciprocal temperature, T^{-1} (Arrhenius-like plots), are presented in Figures 7 and 8, respectively. From Figures 5−8 it can be seen that the pressure and temperature dependences within the ranges 0.1−150 MPa and 20−85 °C (293−358 K) can be fitted by linear plots. Therefore, one may assume that the experimental volumes and enthalpies of activation, deduced from these dependences (eqs 4 and 5, respectively) are approximately constant within the selected pressure and temperature ranges of the present study (see further discussion). The resulting values of ΔV^*_{EXP}, ΔV^*_{Diff}, ΔH^*_{EXP}, and ΔH^*_{Diff} are collected in Table 2. The values for

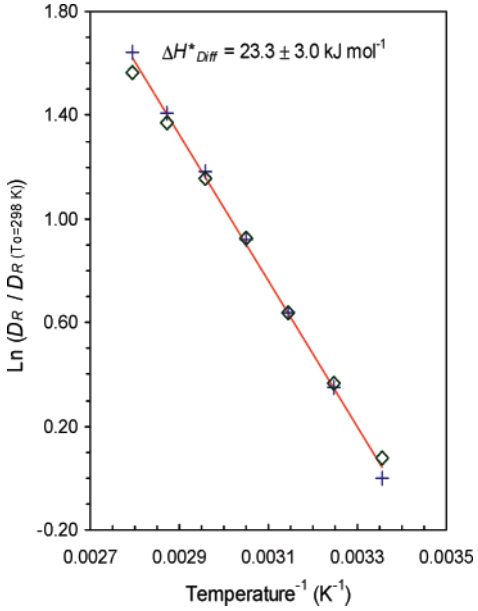

Figure 8. Temperature effect on the diffusion coefficient for $[Fe(bipy)_3]^{3+/2+}$ (crosses) and $[Fe(cp)_2]^{+/0}$ (rhombs) electron exchange at the Au electrode in the ionic liquid [BMIM][BTA] at ambient pressure.

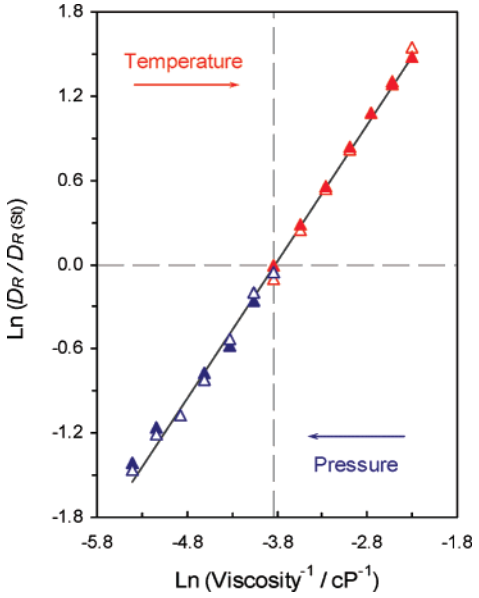

Figure 9. Logarithmic plots of diffusion coefficients for $[Fe(bipy)_3]^{3+/2+}$ and $[Fe(cp)_2]^{+/0}$ in [BMIM][BTA] (closed and open triangles, respectively) versus the solution viscosity as changed through the variation of pressure (this work) and temperature (Okoturo and Van der Noot[31]).

ΔV^*_{EXP} and ΔH^*_{EXP}, as well as for ΔV^*_{Diff} and ΔH^*_{Diff}, related to k^0_{EXP} and D_O, respectively, are virtually the same for the two redox couples studied. Moreover, remarkably, the values of ΔV^* and ΔH^* for the ET and diffusion events were found to be almost the same (Table 2) within the experimental errors (on average, $\pm 1-2$ cm^3 mol^{-1} and $\pm 1-2$ kJ mol^{-1}, respectively), and to closely match the values of $\Delta V^*_{Flu} = +26.9 \pm 0.3$ cm^3 mol^{-1} (this work) and $\Delta H^*_{Flu} = 24.2 \pm 0.5$ kJ mol^{-1} (taken from ref 31). These facts seem to be of exceptional importance if one bears in mind that ΔV^*_{EXP} and ΔH^*_{EXP} represent the genuine heterogeneous ET constants (as rigorously justified above), and, according to eqs 1, 2, 4, and 5, each of them may include contributions from at least three exponential terms, such as ΔV_A, $\Delta V^*\nu_{eff}$ (equivalent to ΔV^*_{Flu}), ΔV^*_{FC} (equivalent to 1/4 ΔV^*_λ), and ΔH_A, $\Delta H^*\nu_{eff}$ (equivalent to ΔH^*_{Flu}), ΔH^*_{FC} (equivalent to 1/4 ΔH^*_λ), respectively. Let us consider the situation in more detail.

Generally, for molecular liquids[29a] and RTILs as well,[29b,c] the Stokes−Einstein equation is applicable, at least semiquantitatively (eq 13):

$$D = \frac{k_B T}{a\pi r\eta} \tag{13}$$

where D is a diffusion coefficient of either the solvent's constituent molecule (ion) or the dissolved reactant species, provided that the latter is of a comparable size to the constituent species, η is the solvent (solution) viscosity, a is an adjustable parameter within the range of 4−6, and r is the Stokes radius of a diffusing species. At the same time, for the effective frequency (eq 2), it has been established that, in the case of solvent dynamic control, eq 3 usually is applicable.[4−8] Actually, the first theoretical work that considered the dynamic solvent control mechanism for ET focused on the Debye-type solvent reorientational relaxation as a main source contributing to ν_{eff}, and, hence, controlling ET according to eq 2, where ν_{eff} is defined through eq 14:[4−8]

$$\nu_{eff} = \nu_L = \tau_L^{-1} = \left(\frac{\epsilon_S}{\epsilon_\infty}\right)\frac{k_B T}{3V_m\eta} \tag{14}$$

Here V_m represents the molar volume, and τ_L is the longitudinal relaxation time that is connected with the Debye relaxation time via the static and infinite dielectric constants, ϵ_S and ϵ_∞. Later this model was extended, allowing for two or more relaxation times,[4c] continuous distribution of these,[30] as well as translational motion (diffusion) of solvent dipoles [4c,18] to contribute to ν_{eff} (see below for extended discussion of the latter case). In any event, according to the well documented theoretical notions[4−6,18,19] and experimental findings,[6−8] the full adiabatic regime would lead to the inverse dependence of the intrinsic ET rate constant on the solvent (solution) viscosity, eq 3 (with $\delta = 1$). Hence, it was crucial to look for direct correlations between the values of CT kinetic constants (as well as diffusion coefficients) and solution viscosity, all variable within the same ranges of pressure and temperature (note that diffusion coefficients of reactants, which, in general, are expected to be linked to the solution viscosity, should not necessarily satisfy eq 13, which implies self-diffusion). For this purpose, we plotted in Figures 9 and 10 the logarithmic dependencies of k^*_{EXP} and D_R altogether as a function of reciprocal viscosity (fluidity), simultaneously including both pressure and temperature portions. The corresponding values of fluidity as a function of pressure were taken from data obtained in the present study (interpolated values from Figure 4 and Table S4). The values for fluidity as a function of temperature are readily available,[22b,31] and, in this particular case, we used the interpolated values derived from the published numerical data of ref 31. The values of k^*_{EXP} and D_R were reduced to the corresponding standard values, which, for technical reasons, were not the same for the pressure and temperature series of experiments. Also, we did not attempt to make corrections because of the temperature multiplication factor in eq 13, for two reasons: (a) the temperature dependence of each of the parameters (eq 5) is known to be strongly affected by the presence of aqueous impurities, which may vary from sample to sample (see Experimental Section for our evaluation); (b) even small unspecified deviations from the Stokes−Einstein law (eq 13) due to "local" viscosity effects[8b,29] may obscure

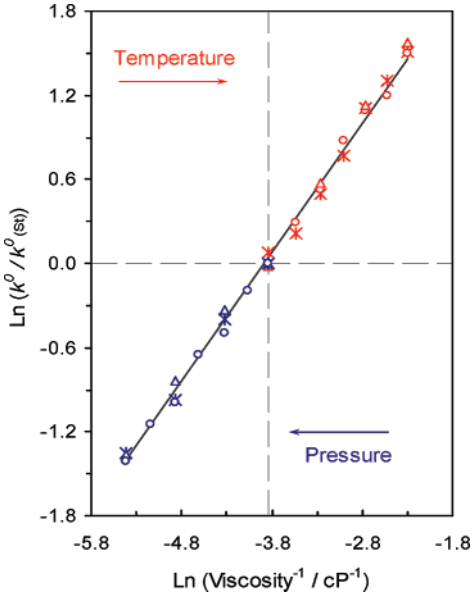

Figure 10. Logarithmic plots of standard rate constants for $[Fe(bipy)_3]^{3+/2+}$ and $[Fe(cp)_2]^{+/0}$ in [BMIM][BTA] (circles/asterisks and triangles, respectively) versus the solution viscosity as changed through the variation of pressure (this work) and temperature (Okoturo and Van der Noot[31]).

the actual picture; hence, a very scrupulous quantitative resemblance of results obtained in different laboratories seemed less meaningful.

Nevertheless, Figure 9 shows, overall, a perfect single correlation between the diffusion coefficients of reactant species and the fluidity of [BMIM][BTA], under variable pressure (at constant temperature) and temperature (at constant pressure) conditions. When the parameter D_R for both redox species is reduced to the corresponding standard values (Table 1), all the data can be approximated by a single linear plot with a slope of 0.98 ± 0.05. Although, as mentioned, a general correlation of this kind could be expected on the grounds of eq 13, the overall span of a 20-fold change in the concerned parameters seems impressive. Even more impressive is the logarithmic dependence of the reduced rate constants on the fluidity of [BMIM][BTA], under variable pressure and temperature conditions (Figure 10). *The CT rate constant (unequivocally reflecting the true CT event) exhibits an unique correlation with the ionic liquid fluidity, notwithstanding the method of viscosity variation*, with an average slope of 0.90 ± 0.05. These plots provide a further visualization of the actual closeness of volumes and enthalpies of activation for k^*_{EXP} and D_R and respective parameters for fluidity. These results in light of earlier theoretical and experimental work, especially by Matsumoto and Swaddle,[10a] obtained for a series of electrode ET in organic molecular liquids involving the representative redox couple, $[Fe(Me_5cp)_2]^{+/0}$, *can be considered as direct and strong evidence for the validity of the solvent dynamic control (fully adiabatic) mechanism* operating through eq 2. This conclusion seemingly is model-free in the sense that it emerges whatever relaxation motion in [BMIM][BTA] controls the CT process (*vide infra*), and automatically brings us to the inference that $\Delta V_A \approx 0$ and $\Delta V^*_{FC} \approx 0$. Deviation of the slope for k^*_{EXP} vs fluidity from unity (Figure 10) can be due to some additional (although minor) kinetic factor contributing to the CT event (*vide infra*). We recall that the latter contribution comes from the Franck−Condon exponential term of eq 2, in which, according to the Marcus theory,[32] eq 15 is validated:

$$\Delta G^*_{ET} = \Delta G_a = \frac{(\lambda - \Delta G_o)^2}{4\lambda} - H_{if} \qquad (15)$$

where ΔG_o is essentially zero throughout our experimental conditions (*vide supra*), yielding $\Delta G_a = \lambda/4 - H_{if}$. We note that the intrinsic enthalpy of activation for the ET process that is determined from the Arrhenius-like treatment (eq 5) is very close to the free energy of activation defined by eq 15, since the intrinsic entropy of activation is usually small (*vide infra*).[6c,9b]

Turning to the pressure effects, for a contribution to the overall activation volume emerging from the Franck−Condon term alone (eq 2), one can derive eq 16 (via eq 4; see refs 2d and 11 for details):

$$\Delta V^*_{FC} = \frac{1}{4}\left(\frac{\partial\lambda}{\partial P}\right)_T - \frac{\partial(H_{if})}{\partial P} \qquad (16)$$

However, it was concluded above that the total value of this term is negligible. A reasonable explanation of this finding is that the two constituent terms, $1/4\ \lambda$ and H_{if}, are of very similar value, and so are their pressure derivative terms. We also note that an advanced expression that substitutes eq 15 leads, in our case, to the result $\Delta G_a = \lambda/4 - H_{if} + (H_{if})^2/\lambda$.[9,32b] However, the latter minor correction does not affect the main conclusion reached in this section.

The closeness of the terms $1/4\ \lambda$ and H_{if} (or $H_{if} - (H_{if})^2/\lambda$), for the case of fully adiabatic electrode reactions (especially when the reactant inner-sphere reorganization contribution is negligible), is not surprising since the value of H_{if} is close to its maximum, H^0_{if}, on average approaching 650 cm^{-1} (8 kJ mol^{-1}),[2b,9,32b] because of the reactant's nearly close approach to the surface of a bare electrode (taking into account an average distance of the reactant particle from the electrode of ca. 3−4 Å due to its own radius, and implying the non-insulating compact part of the double-layer). The classical model of Marcus and its variants have so far predicted the reduction of λ by ca. 20% while approaching the electrode as a result of the increased influence of the image effects.[2b,9,32] On the other hand, in the framework of his extended model, Zusman[4b−d] demonstrated that, when the solution subsystem that undergoes reorganization in the course of ET consists of slower (relaxational) and fast (elastic) degrees of freedom, the solvent control mechanism will be realized as a prevailing motion of the reactive system along the slower reaction coordinate. Therefore, the part of the activation barrier connected with fast variables (the major part of the Marcus reorganization energy, λ) is turned off.[4b,d] Interestingly, Fawcett and Blum[33] (see also ref 6c), upon analyzing a series of ET processes at bare electrodes, came to the conclusion that the "classical" Marcus model largely overestimates the values of λ (as far as processes under solvent dynamic control are considered). The mean spherical approximation (MSA) was applied to estimate the low-frequency contribution to λ, the value of which was found to better resemble that extracted from the experiment. We argue that this contribution is nothing else than the one predicted by Zusman on more general grounds.[4c,d] Indeed, remarkable experiments by Miller et al.[34] upon examining values of λ for ET processes involving different redox species in aqueous media at electrodes modified with *thick* insulator films (SAMs), clearly showed that, at the onset of the non-adiabatic (long-range tunneling) mechanism, the complete Marcus reorganization energy[32,35] fully restores. Finally, in earlier work[2b,36] some of us demonstrated that the value of λ for electrode ET of the redox couple

TABLE 2: Activation Volumes and Enthalpies Obtained from the Pressure and Temperature Dependences of Heterogeneous Standard Rate Constants and Diffusion Coefficients for the $[Fe(bipy)_3]^{3+/2+}$ and $[Fe(cp)_2]^{+/0}$ Redox Couples[a]

redox couple	ΔV^*_{EXP} $cm^3\ mol^{-1}$	ΔV^*_{Diff} $cm^3\ mol^{-1}$	ΔH^*_{EXP} $kJ\ mol^{-1}$	ΔH^*_{Diff} $kJ\ mol^{-1}$
$[Fe(bipy)_3]^{3+/2+}$	$+23.5 \pm 0.8$	$+25.2 \pm 1.5$	23.2 ± 1.2	23.9 ± 1.5
$[Fe(cp)_2]^{+/0}$	$+22.9 \pm 0.8$	$+23.5 \pm 1.5$	22.5 ± 1.2 (23.6 ± 1.2)*	22.4 ± 1.5
average values (as in matching figures)	$+23.2 \pm 1.6$	$+24.4 \pm 3.0$	22.8 ± 2.4	23.3 ± 3.0

[a] Au electrode throughout, except the value for an GC electrode depicted in the fourth column in brackets, denoted by an asterisk.

$[Fe(CN)_6]^{3-/4-}$ at bare Pt and Au in aqueous solutions amounts to ca. 34 kJ mol^{-1}, i.e., to only about 50% of that predicted by conventional theoretical models.[2b,32,33,35] Such a value for λ yields a value of about 8−9 kJ mol^{-1} for $\lambda/4$, and the overall value of $0 \leq \Delta G^*_a = \Delta G^*_{FC} \leq 2$ kJ mol^{-1}. For the redox couple $[Fe(bipy)_3]^{3+/2+}$ in aqueous solutions, the value of λ was found to be even smaller (by ca. 50%) when these two redox couples are compared in the non-adiabatic, i.e., fully accomplished regime.[34] Hence, our reasoning should be valid even to a higher extent for the present case (i.e., for the $[Fe(bipy)_3]^{3+/2+}$ and $[Fe(cp)_2]^{+/0}$ couples in RTIL). On this ground, we propose that the corresponding enthalpy term, ΔH^*_{FC}, like the term ΔV^*_{FC}, in the case of our system, should be negligible within the range of experimental uncertainty. The comparison of experimental values for ΔH^*_{EXP}, and ΔH^*_{Diff} also supports this conclusion regarding the operative solvent dynamic control mechanism that is accompanied by a minimization of the Marcus reorganization energy barrier (Franck−Condon exponential term) and its role in activation volume and enthalpy in the intrinsic CT process (see ref 9 for related discussions). In the next subsection (3.B) we attempt to identify the slow relaxation process that controls the adiabatic CT in the RTIL, and in subsection 3.C we consider how general the conclusions about the microscopic details for ET processes proceeding at bare metal electrodes are in RTILs and also in molecular liquids.

B. The Nature of Slow Relaxation that Controls Adiabatic CT in RTIL. The general condition for the applicability of eq 2 (for a "true" dynamic solvent-controlled ET rate constant) is given in eq 17:[2c,d,4,5]

$$g = \frac{\pi^3 RT(H_{if})^2 \rho_m}{\hbar \nu_{eff} \lambda} \gg 1 \qquad (17)$$

where $\hbar$ is the Planck constant and ρ_m is the density of electronic states in the metal (electrode). As a matter of illustration, for electron exchange at bare Au electrodes, the bulk longitudinal relaxation times for various pure solvents fall within the range $\nu_{eff} \sim 3.3 \times 10^{10}$ to 4.5×10^{12} s^{-1} [37] (including 5×10^{11} s^{-1} for water[37a]). Taking now the most realistic values of other key parameters: $H_{if} \sim 4$ to 20 kJ mol^{-1},[2b,9] $\lambda \sim 20$ to 34 kJ mol^{-1},[2b,36] (*vide supra*), and $\rho_m \approx 3 \times 10^{-3}$ kJ^{-1} mol,[2b,38] one obtains $g = (20-150) \gg 1$, for these particular, or any other reasonably selected parameters, predictive of the solvent friction (adiabatic) mechanism for electrochemical CT. Later, Zusman[4d,18] introduced an alternative extended theoretical model in which the translational motion of dipolar solvent molecules (constituents of molecular liquids) may cause a major contribution to ν_{eff}. The corresponding input can be expressed by eq 18:

$$\tilde{\nu}_{eff} = \left(\frac{\epsilon_s}{\epsilon_\infty}\right) Df(R_e) \qquad (18)$$

where $f(R_e)$, in general, is a smooth function of the CT distance and some other geometrical characteristics such as the reactants effective radius.[4d,18] From the further implicit extension of this model, in the spirit of ref 4d, it also follows that, under certain conditions, any kind of diffusional relaxation occurring in a given molecular or ionic liquid that correlates with the solvent (solution) viscosity (through eqs 14 or 18) may control adiabatic CT (*vide infra*). In other words, *the correlation of the rate constant (in a true kinetic regime) with the solvent (solution) viscosity with a high degree of confidence indicates the solvent control mechanism, but not necessarily by ("slow") reorientational relaxation.*

Murray et al.[21] have suggested that, in viscous fluids rich in ionic components, ion diffusion may be the slowest microscopic event that determines homogeneous or heterogeneous CT (see also ref 19). However, these authors rejected (or ignored) the solvent dynamic control mechanism favoring one that can be viewed as some sort of "diffusionally gated" mechanism (*vide infra*). The question concerning the possible decisive role of slow ionic motion so far has not appeared regarding "true" adiabatic ET. Importantly, as mentioned in the Introduction, numerical details of the Debye-type relaxation for various molecular liquids that are used for the quantification of CT expressions such as eq 2 are commonly obtained through the method of dielectric relaxation spectroscopy (DRS), for which, in the case of pure substances, translational (diffusion) modes do not contribute to the dielectric polarization.[17] Similar data for molecular liquids containing high concentrations of electrolytes, providing some information about the diffusion modes of dissolved ions, are rarely available. Meanwhile, electrochemical experiments exploiting common molecular liquids (water, organic substances) as solvents always employ substantial concentrations of supporting electrolytes in order to provide sufficient conductivity.[1a,b] The ionic components of dissolved electrolytes form an inhomogeneous immediate environment for the "reaction zone" in which the actual ET takes place.[2b,6−8] The diffusive motions of the electrolyte ions (which could be cations or anions, depending on the charged state of the electrode and the degree of its specific interaction with ions) are almost frozen in the compact part of the double layer, and should be significantly slowed down in the layer next to the compact part (that is, the diffusive part normally encountered in conventional electrolyte solutions, which is the intermediate region between the compact layer and the bulk solution).[1a,2b] This pattern is somewhat similar to the one encountered and broadly discussed in the case of water/biomacromolecule interfaces for globular proteins.[2d,39] Consequently, the slow translational motion of component ions may be a source for frictional restrain in the framework of a "modified" solvent dynamic control mechanism. Actually, in the case of "common" solutions (including molecular solvents and dissolved electrolytes) the motion of solvent molecules and dissolved ions should be strongly coupled, especially in the relatively more viscous (compared to the bulk), slowly relaxing, diffusive-like part of the double layer.

The RTILs offer the exceptional opportunity for in-depth studies of the adiabatic electrochemical ET, regarding the

identification of the dominant relaxation process contributing to ν_{eff} (at least, for this type of solvents; see subsection 3.C). These substances seem to be especially convenient because they exist as "solvent-free", highly concentrated, liquid electrolytes that should simplify the double-layer structure at least as a result of its natural "homogeneity" (thanks to the avoidance of solvent−solute local inhomogeneity or "mixing"). Indeed, for RTILs that are related to ours, it has been shown by recent experimental[16a,b] and molecular dynamics simulation studies[16c,d] that, presumably, within the whole potential range of the present interest (−0.2 to 1.3 V, vs Ag wire), the BTA anions prevailingly should form a rather compact (plausibly lattice-like) part of the double layer. This compact layer cannot be used by the present redox couples as reactive sites (a) because this zone is already occupied (in a statistical sense) by the BTA anions; and (b) because of the electrostatic repulsion of, on the average, positively charged reactants from the electrode. Obviously, the layer next to the compact one should be rich in BMIM cations and less structured (experiencing higher diffusional mobility; this zone in some terms is analogous to the diffusive part of the double layer for the electrode/conventional electrolyte solution junctions) compared to the former one. This region of the double layer could easily serve as a reactive zone for both kinds of redox species exploited in our work (note, in contrast to conventional electrolyte solutions, for the case of charged surface/ILs interfaces one should expect directional oscillations of the excess ion extent, spanning a few layers[16c,d]). Therefore, for RTILs, in fact, involvement of corresponding translational (diffusional) modes in a frictional relaxation arises automatically. This detail may serve as a key aspect for further insight into the microscopic mechanism.

Let us attempt to identify the slowest relaxation motion that controls the CT rate process in electrochemical systems (eqs 1 and 2). A similar problem of the identification of a slow (controlling) mode emerged in the earlier work[9] for short-range (adiabatic) electrode CT to/from redox species covalently tailored to *thin* alkanethiol SAMs. As already mentioned above, it is generally accepted, and will also be assumed for this particular case (implying reactants' free diffusion), that $\delta R_e = 2 \times 10^{-9}$ to 10^{-8} cm, and $\Delta G_A \approx 0$. Also, $\Delta G^*_a \leq RT$ and $\lambda \leq 34$ kJ mol^{-1} (*vide supra*). These values, along with the average experimental value of $k^0_{EXP} = 2 \times 10^{-3}$ cm s^{-1}, allow one to deduce the actual value of $\nu_{eff} = 10^9$ to 10^{10} s^{-1}. Analysis of the relevant literature reveals that, for RTILs, including [BMIM][BTA], a very broad spectrum of relaxational events within the time-domain from subpicoseconds to tens and even hundreds of nanoseconds have been identified by different methods. Dielectric spectroscopy[17] and dynamic solvation[40] data are available in the literature that could be ascribed to the rotational motion of constituent ions in different RTILs, including [BMIM][BTA]. These fall within the range of characteristic times of 1−100 ps (yielding $\nu_{eff} = 10^{10}-10^{12}$ s^{-1}). Obviously, this kind of motion is not slow enough to provide the observed high friction (estimated through the set of experimental and accurately predicted parameters, using eqs 1 and 2). However, the slowest relaxation times detected by experimental techniques fall within the "tail" of a spectrum (which is well described by the stretched exponential function) that "locks" the overall broad distribution of relaxation times.[40] As mentioned by Hu and Margulis,[41] in subsequent studies of time-dependent fluorescence of dipolar molecules in imidazolium-based RTILs (such as [BMIM][BTA]), the fluorescent probe 2-amino-7-nitrofluorene (ANF), exhibits an excitation-wavelength-dependent fluorescent spectrum (the so-called "red-edge effect"). This effect can be explained on the basis of a much longer time-scale of solvent (RTIL) relaxation compared to the lifetime of the ANF excited state, which is about 100 ps. According to further work by Hu and Margulis,[40d] the full energy relaxation upon photoexcitation (or, in the course of ET, as in the present case) must be compatible with the time-scale on which the solute (or solvent) ion abandons the cage regime and enters into the diffusion (displacement) regime. Certainly, a large part of the relaxation after photoexcitation occurs on the short subpicosecond and picosecond time scale.[40] In terms of the theory of CT, these time domains correspond to fast degrees of freedom contributing to the "full" Marcus reorganization free energy (*vide supra*). According to the computational work by Hu and Margulis,[41] under ambient conditions (300 K, 0.1 MPa), the characteristic time for the square displacement of ca. 1 Å^2 that still has sufficiently high probability, approaches the time domain of ca. 10 ns. We conclude that, at the RTIL/electrode interface, in a diffusive part of the interfacial double layer (in which most probably the reaction zone is located), the ion displacement (diffusional relaxation) characteristic time may increase to 50−100 ns, which is more than enough time to account for the "slow" dynamic control comprehended above.

C. Further Insight into the Microscopic Mechanisms of Diffusion and CT at Bare Metal Electrodes. We arrived at the conclusion that, most probably, translational motion (diffusion) of constituent ions of the solvent (RTIL) in the vicinity of the reaction zone near the electrode should be the major source that determines the value of the key parameter, ν_{eff}, and, hence, of the adiabatic rate constant (eq 2). We now recall the fact that the values of the activation volume and enthalpy for this ET and the reactants diffusion (from the bulk solvent to the reaction zone) are virtually equal (see Table 2), and attempt to explain this equity for the underlying processes on a general basis. Considering the values for the volumes of activation, $\Delta V^*_{EXP} \approx \Delta V^*_{ET} \approx \Delta V^*_{Flu} \approx \Delta V^*_{Diff}$, it is reasonable to relate them to a new space (hole) that should be formed in the microscopic process of the displacement stage, implying either the diffusional motion of the reactant particle itself, or the diffusional motion of the solvent constituting ions responsible for a frictional control. However, this value (∼23 cm^3 mol^{-1}, for the two studied processes in [BMIM][BTA], Table 2) is only about 5% of the average reactants total volume, and about 13% of the average constituent ions total volume. Obviously, the probability for the formation of volumes as large as 180 (liquid components) or 460 cm^3 mol^{-1} (reactant species), either in pre-equilibrium or in the transition state, is extremely low. Consequently, it is logical to suppose that the experimentally observed volume of activation corresponds to the elementary volume that can be "created" within the elementary diffusive process. Seemingly, it is independent of the volume of the diffusing species, but is a property of the solvent. The latter interpretation is very close to the notions of the Adam−Gibbs theory[42a] that was first proposed to account for the experimental data for the temperature dependence of different transport properties for conventional glass-forming liquids. According to Adam and Gibbs, one can ascribe our volumes of activation to the "minimal volume cooperatively rearranging region" (for some modern formulations, see refs 42b−d) of the given RTIL or, in a general case, of any kind of molecular or ionic liquid that is a property of the given solvent, but not the diffusing particle (excluding small particles exhibiting anomalous diffusion).

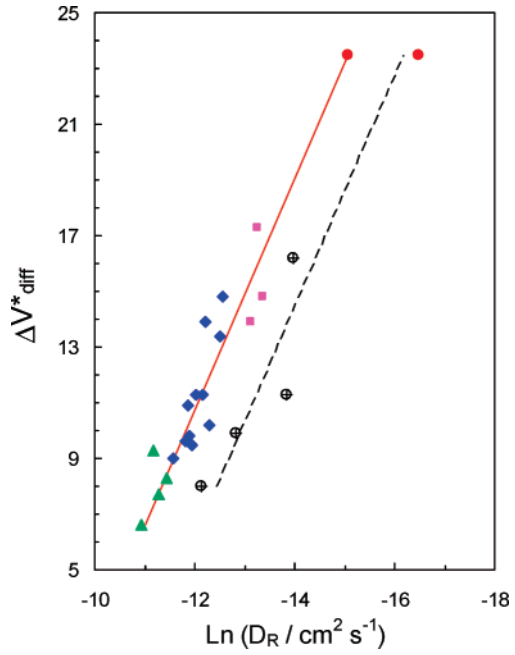

Figure 11. A plot of the activation volumes, ΔV^*_{Diff}, versus the corresponding diffusion coefficients for the following redox couples: decamethylferrocene ($[Fe(Me_5cp)_2]^{+/0}$), $[Fe(cp)_2]^{+/0}$ (filled triangles, rhombs, and squares) and iron trisphenanthroline ($[Fe(phen)_3]^{3+/2+}$) (circles with crosses inside) obtained within a series of typical organic liquids.[10a] Data from the present study for $[Fe(cp)_2]^{+/0}$ and $[Fe(bipy)_3]^{3+/2+}$ in [BMIM][BTA] (two closed circles at the top) are also included.

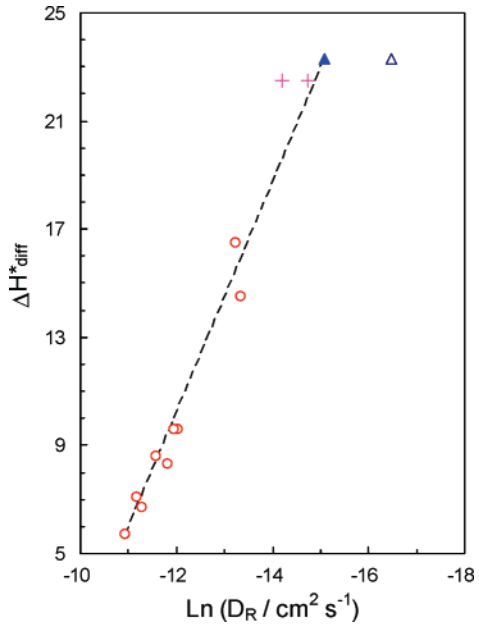

Figure 12. A plot of the activation enthalpies, ΔH^*_{Diff}, versus the corresponding diffusion coefficients for the redox couples of similar charge state $[Fe(Me_5cp)_2]^{+/0}$ (in molecular organic liquids;[10a] open circles) and $[Fe(cp)_2]^{+/0}$ (in [BMIM][BTA]) (present work, closed triangle at the top; open triangle represents $[Fe(bipy)_3]^{3+/2+}$). Literature data for the self-diffusion coefficients of the component ions of [BMIM][BTA][29a] are also included (crosses).

It seems interesting now to compare the results of the present study on the volumes and enthalpies of activation with those obtained earlier for the series of organic molecular liquids. We only consider data for the diffusion coefficients, since the earlier enthalpy data for the ET rate constants[10a] are complicated by the temperature-sensitive double-layer effects, making these data less reliable (*vide infra*). In Figure 11 the data of Matsumoto and Swaddle[10b] for activation volumes, ΔV^*_{Diff}, are plotted versus the corresponding diffusion coefficients for the redox couples decamethylferrocene ($[Fe(Me_5cp)_2]^{+/0}$), $[Fe(cp)_2]^{+/0}$, and iron trisphenanthroline ($[Fe(phen)_3]^{3+/2+}$) obtained within the series of typical organic liquids. For comparison, our data from the present study for $[Fe(cp)_2]^{+/0}$ and $[Fe(bipy)_3]^{3+/2+}$ in [BMIM]-[BTA] are also included. From Figure 11 it can be concluded that, despite pronounced scatter, the data obtained for [BMIM]-[BTA] fall on the same overall dependence formed by the series of molecular organic liquids (some of them represent data obtained at different concentrations of supporting electrolytes, in total 22 experimental points[10a]). Obviously, the redox couples—$[Fe(Me_5cp)_2]^{+/0}$ together with $[Fe(cp)_2]^{+/0}$, and $[Fe(phen)_3]^{3+/2+}$ together with $[Fe(bipy)_3]^{3+/2+}$—form different arms of this dependence, despite the difference in the reactant size and geometry. We now turn to the enthalpy of activation and consider Figure 12, which represents the dependence of ΔH^*_{Diff} on the corresponding diffusion coefficients for redox couples of similar charge state $[Fe(Me_5cp)_2]^{+/0}$ (in molecular organic liquids) and $[Fe(cp)_2]^{+/0}$ (in [BMIM][BTA]). For comparison, the literature data for the self-diffusion coefficients of component ions of [BMIM][BTA] are also included (crosses).[29a] Analogously to Figure 11, the data obtained for [BMIM][BTA] again fall on the same overall dependence formed by the series of molecular organic liquids. From these observations we conclude with a high probability that the mechanism of the elementary diffusion stage in molecular liquids and RTILs is the same and is determined by the formation of the "minimal cooperatively rearranging region", which is mainly a property of the given solvent. It can be seen that the value of ΔV^*_{Diff} always remains much smaller (2.5 to 5%) compared to the average molar volume of the diffusing reactant ion as well as the solvent components. Interestingly, the reactant charge state does not play a role in determining the parameters ΔV^*_{Diff} and ΔH^*_{Diff}. However, the probability of an elementary diffusion stage seems to depend on the charge state of the diffusing particle. Obviously, dipole−dipole, ion−dipole, or ion−ion interactions are important for the determination of the probability and, hence, the entropy of activation of the elementary diffusing stage.

We also compared the performance of activation enthalpies for the CT processes in organic molecular liquids and in [BMIM][BTA]. From the high-pressure kinetic studies we obtained that, in [BMIM][BTA], $\Delta V^*_{EXP} \approx (\Delta V^*_{ET}) \approx (\Delta V^*_{Flu}) \approx \Delta V^*_{Diff}$. The same was found by Matsumoto and Swaddle[10a] for a series of organic molecular liquids. However, in the case of [BMIM][BTA], we also found that $\Delta H^*_{EXP} \approx (\Delta H^*_{ET}) \approx (\Delta H^*_{Flu}) \approx \Delta H^*_{Diff}$. We consider both observations as direct proof for the validation of the dynamic solvent control mechanism with the additional deduction that $\Delta V_A \approx 0$ and $\Delta V^*_{FC} \approx 0$, and $\Delta H_A \approx 0$ and $\Delta H^*_{FC} \approx 0$. At the same time, Matsumoto and Swaddle[10a] found that, within the series of organic molecular liquids, there is always the following inequity: $\Delta H^*_{EXP} > \Delta H^*_{Diff}$. This fact was interpreted as an indication for $\Delta H^*_{FC} \gg 0$. However, the same authors outlined that the double-layer effects may largely interfere with kinetic data in terms of temperature effects. Indeed, we found that the value of ΔH^*_{EXP} in the case of molecular liquids often largely depends on the concentration of the supporting electrolyte applied,[10a] which is a reasonable indication of the role of the double-layer motif. Hence, we conclude that, in that case, $\Delta H_A \gg 0$ and, still, $\Delta H^*_{FC} \approx 0$. This simply means that the elementary outer-sphere (uncomplicated) CT process at bare metal electrodes, independently of the solvent nature (molecular

TABLE 3: Experimental Cell Volumes (ΔV_{Cell}), Entropies (ΔS_{Cell}), Reference Electrode Volumes (ΔV_{Ref}), Entropies (ΔS_{Ref}), and Evaluated Volumes (ΔV_{Elec}), Entropies (ΔS_{Elec}), and Enthalpies (ΔH_{Elec})[a,b]

redox couple	ΔV^0_{Cell} cm^3 mol^{-1}	ΔV^0_{Ref} cm^3 mol^{-1}	ΔV^0_{Elec} cm^3 mol^{-1}	ΔS^0_{Cell} J mol^{-1} K^{-1}	ΔS^0_{Ref} J mol^{-1} K^{-1}	ΔS^0_{Elec} J mol^{-1} K^{-1}	ΔH^0_{Elec}[a] kJ mol^{-1}
$[Fe(bipy)_3]^{3+/2+}$	+10.5	−15.0	+25.5	+94.9	−83	+178	+53
		(−10.0)[b]	(+20.5)[b]		(−49)[c]	(+144)[c]	(+43)[c]
$[Fe(cp)_2]^{+/0}$	−6.0	−15.0	+9.0	−20.1	−83	+63	+18.8
		(−10.0)[b]	(+4.0)[b]		(−49)[c]	(+29)[c]	(+8.7)[c]

[a] The latter three are due to solvent electrostriction for the $[Fe(bipy)_3]^{3+/2+}$ and $[Fe(cp)_2]^{+/0}$ redox couples in [BMIM][BTA] detected by the bare Au electrode. The data rows are obtained through eqs 19 and 24 using crystallographic values for r. [b] The values obtained from the condition $\Delta G^0_{Elec} = \Delta G^0 = 0$, i.e., $\Delta H^0_{Elec} = T\Delta S^0_{Elec}$ (see text for details). [c] Obtained by using eq 19 with r considered as a constant (see text for details). [d] Obtained by using eq 24 with r considered as a constant (see text for details).

liquids versus RTILs), takes place through the fully adiabatic mechanism in which the Marcus barrier is almost totally diminished. The apparent excess enthalpies of activation arise from nonzero pre-equilibrium enthalpies due to the unfavorable interactions of reactant species in the double-layer. These interactions are seemingly not connected with the pre-equilibrium volume changes.

In contrast to molecular liquids,[1] in the case of [BMIM]-[BTA], the structure of the double-layer is more rationally tractable,[16] at least within the potential range of our present interest, −0.2 to 1.3 V, vs Ag wire (at least 0.3 V above the proposed potential of zero charge[16b]). Therefore, penetration of the reactant ion into the diffusive-like part of the double-layer (*vide infra*) may not be connected with either the enthalpy or the volume changes. Hence the RTILs appear to be more convenient media for the verification of microscopic CT mechanisms regarding their adiabaticity and the role of the Franck−Condon factor. Another significant purpose of studying CT in RTILs is that it revealed a possible analogy with molecular liquids regarding both the microscopic diffusional and ET stages, particularly of the microscopic process underlying the frictional control. In light of the present work, it appears likely that the slow ionic diffusion of electrolyte components, not the bulk Debye relaxation of solvent dipoles, determines dynamic "solvent" control in the adiabatic regime for most electrochemical processes.

D. Impact of Pressure and Temperature on $E^0_{1/2}$. Another interesting aspect of the application of pressure and temperature variation is connected with the equilibrium properties of ET. The primary task of the present investigation was an in-depth study of the intrinsic CT mechanism in RTIL. From the pressure and temperature dependence of the formal redox potentials, $E^0_{1/2}$, (which can be associated with the peak midpoint potential of the reversible CV signal[1a]) attained for two redox couples of different charge type, the values of the intrinsic electrostrictive thermodynamic parameters such as ΔV^0_{Elec} and ΔS^0_{Elec} could be estimated.[43,44] This is valuable information on the volume and entropy changes that result for ion solvation accompanying the net change in charge during ET. Thus, in principle, some connection between the intrinsic equilibrium and dynamic patterns of CT, especially for the new type of solvents such as RTIL, can be elucidated.

In the context of pressure dependence studies, the volume change due to ion−solvent interaction upon CT (i.e., the half-cell reaction volume) through the application of the Drude−Nernst relationship is given by eq 19:[43]

$$\Delta V^0_{Elec} = -\frac{B}{r}(z_{ox}{}^2 - z_{red}{}^2) = -\frac{B(\Delta z^2)}{r} \qquad (19)$$

where Δz^2 is the change in the square of the ionic charge due to ET, r_{eff} is the effective ion radius, and B is a constant independent of the ion's charge state. At the same time, the value of ΔV^0_{Elec} is part of the experimentally determinable cell reaction volume, ΔV^0_{Cell}, according to eq 20:[43]

$$\Delta V^0_{Cell} = \Delta V^0_{Elec} + \Delta V^0_{Intr} + \Delta V^0_{Ref} \qquad (20)$$

which also includes terms due to intrinsic volume changes arising from the reduction of the complex, ΔV^0_{Intr}, and the reaction volume associated with the oxidation of silver in the reference electrode (the other half-cell reaction), ΔV^0_{Ref}.[43] Figure 13 presents the dependence of the peak midpoint potential deviation from its value under close to ambient conditions (5 MPa, 293 K; see Experimental Section) as a function of pressure, from which the cell reaction volumes for the two redox couples were estimated according to eq 21[43] (see Table 3):

$$\left[\frac{\partial E^0_{1/2}}{\partial P}\right]_T = -\frac{\Delta V^0_{Cell}}{F} \qquad (21)$$

Subsequently, the cell reaction volumes are plotted as a function of $\Delta z^2/r$ for the two couples of different charge state as a linear function (see ref 43). Extrapolation of this dependence to the point where $\Delta z^2 = 0$ allows the estimation of the volume change generated by the reference cell only, ΔV^0_{Ref} (eq 20), provided that, for the redox couples under study, the inner-sphere reorganization, and all its derivatives are of minor importance and hence negligible (in particular, $\Delta V^0_{Intr} \approx 0$).[10b,43,44]

Concerning the role of the ionic radius in eq 19, it turns out to be somewhat ambiguous because earlier numerical estimates of the ionic radii from the Drude−Nernst relationship yield unrealistically high values and show no dependence on the size of the ions.[45] For this reason, previous authors concluded that eq 19 is strictly applicable only regarding the term Δz^2, but not r (i.e., effectively, $\Delta r_{eff} \approx 0$). We plotted the cell reaction volume (ΔV^0_{Cell}) versus the value of $\Delta z^2/r$, and versus Δz^2 alone. The plots were extrapolated to the point where $\Delta z^2 = 0$, and the values of ΔV^0_{Ref} were determined under two different conditions (by considering and neglecting changes in Δr_{eff}, respectively). The corresponding values are collected in Table 3, and the former plot is presented in Figure S4 (Supporting Information). Although the plot is based on only two experimental points, its linear character is justified by earlier work[43] that employed four redox couples of different charge state (in aqueous solution) and demonstrated a perfect linear dependence. Hence, two sets of values for ΔV^0_{Elec} were calculated from eq 20, and are presented in Table 3.

In the context of temperature dependence studies by analogy to eqs 19−21, the equilibrium cell entropy and entropy change due to ion−solvent interaction upon CT can be analyzed with

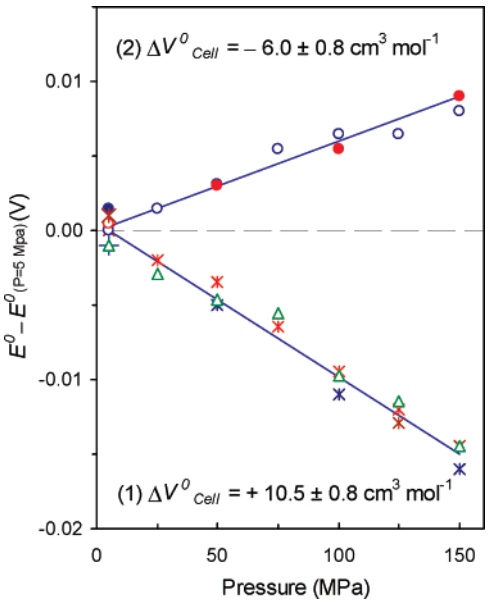

Figure 13. High-pressure effect on (1) $[Fe(bipy)_3]^{3+/2+}$ (crosses/triangles) and (2) $[Fe(cp)_2]^{+/0}$ (circles) electron exchange at the Au electrode in [BMIM][BTA] at 20 °C.

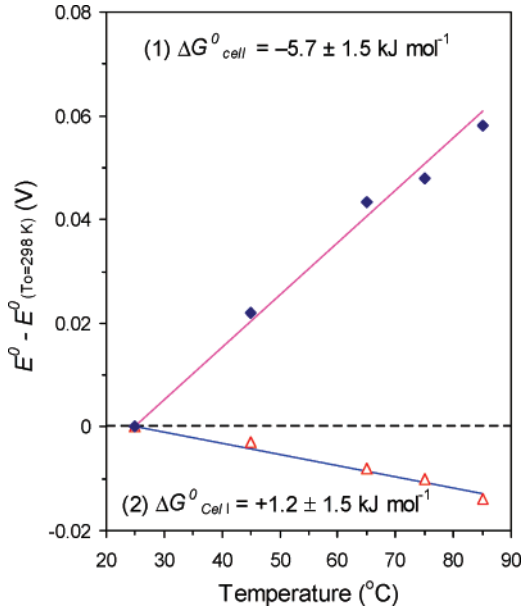

Figure 14. Temperature effect on (1) $[Fe(bipy)_3]^{3+/2+}$ (rhombs) and (2) $[Fe(cp)_2]^{+/0}$ (triangles) electron exchange at the Au electrode in [BMIM][BTA] at ambient pressure.

eqs 22−24, respectively.[10a,44]

$$\left[\frac{\partial E^0_{1/2}}{\partial T}\right]_P = -\frac{\Delta S^0_{Cell}}{F} \quad (22)$$

$$\Delta S^0_{Cell} = \Delta S^0_{Elec} + \Delta S^0_{Intr} + \Delta S^0_{Ref} \quad (23)$$

$$\Delta S^0_{Elec} = -\frac{C}{r}(z_{ox}{}^2 - z_{red}{}^2) = -\frac{C(\Delta z^2)}{r} \quad (24)$$

Figure 14 presents the dependence of the peak midpoint potential deviation from its value under ambient conditions (298 K, 0.1 MPa) as a function of temperature, from which the cell entropies for the two redox couples were estimated according to eq 22[10a] and collected in Table 3. The procedure for the determination of ΔS^0_{Elec} was similar to the one for ΔV^0_{Elec} described above (taking into account that $\Delta S^0_{Intr} \approx 0$). The reference reaction entropy, ΔS^0_{Ref}, was determined in two ways: by plotting the cell reaction entropy versus the value of $\Delta z^2/r$ and versus Δz^2 alone. All the obtained values, including ΔS^0_{Elec}, are collected in Table 3, and the extrapolated plot of ΔS^0_{Cell} versus $\Delta z^2/r$ is presented in Figure S5 (Supporting Information).

In contrast to the case of volume effects, a definite correlation of ΔS^0_{Elec} with r has been demonstrated before for a number of redox couples dissolved in a variety of molecular liquids.[44] Hence, the values of ΔS^0_{Ref} and ΔS^0_{Elec} obtained from the extrapolated plot in Figure S5 seem to be more reliable. In addition, the value of ΔH^0_{Elec} was determined from $\Delta H^0_{Elec} = T\Delta S^0_{Elec}$, under the assumption that $\Delta G^0_{Elec} = \Delta G^0 = 0$ at $E = E^0_{1/2}$ (at ambient pressure conditions). This implies that changes in the electrostatic ion−solvent interactions mainly determine the variation of $E^0_{1/2}$ with temperature (and with pressure, as well). At any temperature or pressure, for each $E^0_{1/2}$, the enthalpy (ΔH^0), entropy ($-T\Delta S^0$), and volume ($P\Delta V^0$) contributions should compensate each other to result in $\Delta G^0 = 0$ for ET to and from the electrode, which is the condition for equilibrium at $E^0_{1/2}$.[1a,b]

To summarize this subsection, we emphasize that, despite some uncertainty in the determination of thermodynamic parameters, the complete equilibrium ET pattern for a given RTIL definitely shows remarkable similarity with that for a variety of molecular liquids.[1c,10a] This similarity is much less vibrant in the case of dynamic patterns displaying only distantly comparable behavior regarding the kinetic parameters for ET and diffusion in ordinary molecular liquids and RTILs.

4. Conclusions

(a) The intrinsic steps of outer-sphere heterogeneous CT involving the $[Fe(bipy)_3]^{3+/2+}$ and $[Fe(cp)_2]^{+/0}$ redox couples at bare Au electrodes in an RTIL, [BMIM][BTA], like the matching short-range electrode processes proceeding in molecular liquids, take place in the full adiabatic (solvent control) regime.

(b) The specific contribution due to the pre-equilibrium term, as well as the dynamic Marcus reorganization component (Franck−Condon factor), introduce minimal (almost diminished) contributions to both the volume and enthalpy of activation determined experimentally through pressure and temperature variations.

(c) The frictional control by solvent most probably takes place through the slow translational dislocations of constituent ions of the RTIL within the diffusive-like part of the metal/solvent interface layer (where the reaction zone is presumably located).

(d) Translational diffusion of both the reactant and solvent constituent ions occurs by a similar mechanism via the creation of the minimal cooperatively rearranging region for which the activation volume and activation enthalpy are the unique properties of the given solvent.

Acknowledgment. The authors gratefully acknowledge financial support from DAAD (Fellowship for T.D.D., 2007), the Alexander von Humboldt Foundation (Resumption of Fellowship for D.E.K., 2005), the Dr. Hertha and Helmut Schmauser Foundation (Fellowship for D.E.K., 2006), and the Deutsche Forschungsgemeinschaft within SFB 583 on "Redox-active Metal Complexes" and SPP 1191 on "Ionic Liquids".

D.E.K. is grateful to Prof. R. G. Compton for helpful comments on a temperature-dependence protocol of the Nicholson method. The density of the ionic liquid as a function of pressure was kindly measured by Tim Predel from the group of Prof. E. Schlücker (Institute for Process Technology and Machinery, University of Erlangen-Nürnberg).

Supporting Information Available: Additional figures and tables referenced in the text. This material is available free of charge via the Internet at http://pubs.acs.org.

References and Notes

(1) (a) Bard, A. J.; Faulkner, L. R. *Electrochemical Methods: Fundamentals and Applications*, 2nd ed.; John Wiley & Sons: New York, 2001. (b) Fawcett, W. R. *Liquids, Solutions and Interfaces*; Oxford University Press: Oxford, 2004. (c) Swaddle, T. W. *Chem. Rev.* **2005**, *105*, 2573−2608.

(2) (a) Finklea H. O. Self-assembled monolayers on electrodes. In *Encyclopedia of Analytical Chemistry*; Meyers, R. A., Ed.; Wiley: Chichester, U.K., 2000; pp 1−29. (b) Khoshtariya, D. E.; Dolidze, T. D.; Zusman, L. D.; Waldeck, D. H. *J. Phys. Chem. A* **2001**, *105*, 1818−1829. (c) Khoshtariya, D. E.; Wei, J.; Liu, H.; Yue, H.; Waldeck, D. H. *J. Am. Chem. Soc.* **2003**, *125*, 7704−7714. (d) Khoshtariya, D. E.; Dolidze, T. D.; Seyfert, S.; Sarauli, D.; Lee, G.; van Eldik, R. *Chem.−Eur. J.* **2006**, *12*, 7041−7056.

(3) (a) Newton, M. D.; Friedman, H. L. *J. Chem. Phys.* **1985**, *83*, 5210−5218. (b) Hupp, J. T.; Weaver, M. J. *J. Electroanal. Chem.* **1983**, *152*, 1−14. (c) Gochev, A.; McManis, G. E.; Weaver, M. J. *J. Chem. Phys.* **1989**, *91*, 906−916. (d) Fawcett, W. R.; Foss, C. A. *J. Electroanal. Chem.* **1989**, *270*, 103−118.

(4) (a) Zusman, L. D. *Chem. Phys.* **1980**, *49*, 295−304. (b) Zusman, L. D. *Chem. Phys.* **1983**, *80*, 29−43. (c) Zusman, L. D. *Chem. Phys.* **1987**, *112*, 53−59. (d) Zusman, L. D. *Z. Phys. Chem.* **1994**, *186*, 1−29.

(5) (a) Calef, D. F.; Wolynes, P. G. *J. Chem. Phys.* **1983**, *78*, 470−482. (b) Morgan, J. D.; Wolynes, P. G. *J. Chem. Phys.* **1987**, *91*, 874−883. (c) Beratan, D. N.; Onuchic, J. N. *J. Chem. Phys.* **1988**, *89*, 6195−6203. (d) Rips, I.; Jortner, J. *J. Chem. Phys.* **1988**, *88*, 167−170. (e) Kosloff, R.; Ratner, M. A. *J. Phys. Chem. B* **2002**, *106*, 8479−8483.

(6) (a) Hines, J. T. *J. Phys. Chem.* **1986**, *90*, 3701−3706. (b) Weaver, M. J.; McManis, G. E. *Acc. Chem. Res.* **1990**, *23*, 294−300. (c) Weaver, M. J. *Chem. Rev.* **1992**, *92*, 463−480. (d) Fawcett, W. R.; Opallo, M. *Angew. Chem., Int. Ed. Engl.* **1994**, *33*, 2131−2143. (e) Bixon, M.; Jortner, J. *Adv. Chem. Phys.* **1999**, *106*, 35−202.

(7) (a) Pyati, R.; Murray, R. W. *J. Am. Chem. Soc.* **1996**, *118*, 1743−1749. (b) Williams, E.; Crooker, J. C.; Pyati, R.; Lyons, L. J.; Murray, R. W. *J. Am. Chem. Soc.* **1997**, *119*, 10249−10259. (c) Winkler, K.; McKnight, N.; Fawcett, W. R. *J. Phys. Chem. B* **2000**, *104*, 3575−3580.

(8) (a) Khoshtariya, D. E.; Dolidze, T. D.; Krulic, D.; Fatouros, N.; Devilliers, D. *J. Phys. Chem. B* **1998**, *102*, 7800−7806. (b) Khoshtariya, D. E.; Dolidze, T. D.; Vertova, A.; Longhi, M.; Rondinini, S. *Electrochem. Commun.* **2003**, *5*, 241−245.

(9) (a) Smalley, J. F.; Finklea, H. O.; Chidsay, C. E. D.; Lindford, M. R.; Creager, S. E.; Ferraris, J. P.; Chalfant, K.; Zawodzinsk, T.; Feldberg, S. W.; Newton, M. D. *J. Am. Chem. Soc.* **2003**, *125*, 2004−2013. (b) Newton, M. D.; Smalley, J. F. *Phys. Chem. Chem. Phys.* **2007**, *9*, 555−572. (c) Smalley, J. F. *J. Phys. Chem. B* **2007**, *111*, 6798−6806.

(10) (a) Matsumoto, M.; Swaddle, T. W. *Inorg. Chem.* **2004**, *43*, 2724−2735. (b) Fu, Y.; Cole, A. S.; Swaddle, T. W. *J. Am. Chem. Soc.* **1999**, *21*, 10410−10415. (c) Matsumoto, M.; Lamprecht, D.; North, M. R.; Swaddle, T. W. *Can. J. Chem.* **2001**, *79*, 1864−1869. (d) Zhou, J.; Swaddle, T. W. *Can. J. Chem.* **2001**, *79*, 841−847.

(11) (a) Dolidze, T. D.; Khoshtariya, D. E.; Waldeck, D. H.; Macyk, J.; van Eldik, R. *J. Phys. Chem. B* **2003**, *107*, 7172−7179. (b) Khoshtariya, D. E.; Dolidze, T. D.; Sarauli, D.; van Eldik, R. *Angew. Chem., Int. Ed.* **2006**, *45*, 277−281.

(12) (a) *Inorganic High-Pressure Chemistry: Kinetics and Mechanisms*; van Eldik, R., Ed.; Elsevier: Amsterdam, 1986. (b) *High Pressure Chemistry*; van Eldik, R., Klärner, F.-G., Eds.; Wiley-VCH: Weinheim, Germany, 2002. (c) van Eldik, R.; Asano, T.; Le Noble, W. J. *Chem. Rev.* **1989**, *89*, 549−688. (d) Drljaca, A.; Hubbard, C.D.; van Eldik, R.; Asano, T.; Basilevsky, M. V.; Le Noble, W. J. *Chem. Rev.* **1998**, *98*, 2167−2290.

(13) (a) Khoshtariya, D. E.; Dolidze, T. D.; Neubrand, A.; van Eldik, R. *J. Mol. Liq.* **2000**, *89*, 127−146. (b) Zahl, A.; van Eldik, R.; Matsumoto, M.; Swaddle, T. W. *Inorg. Chem.* **2003**, *42*, 3718−3722.

(14) (a) Welton, T. *Chem. Rev.* **1999**, *99*, 2071−2084. (b) Handy, S. T. *Chem. Eur. J.* **2003**, *9*, 2938−2944. (c) Buzzeo, M. C.; Evans, R. G.; Compton, R. G. *ChemPhysChem* **2004**, *5*, 1106−1120.

(15) (a) Zhang, J.; Bond, A. J. *Analyst* **2005**, *130*, 1132−1147. (b) Fietkau, N.; Clegg, A D.; Evans, R. G.; Villagrán, C.; Hardacre, C.; Compton, R. G. *ChemPhysChem* **2006**, *7*, 1041−1045. (c) Matsumiya, M.; Terazono, M.; Tokuraku, K. *Electrochim. Acta* **2006**, *51*, 1178−1183.

(16) (a) Rivera-Rubero, S.; Baldelli, S. *J. Phys. Chem. B* **2004**, *108*, 15133−15140. (b) Baldelli, S. *J. Phys. Chem. B* **2005**, *109*, 13049−13051. (c) Pinilla, C.; Del Pópolo, M. G.; Kahanoff, J.; Lynden-Bell, R. M. *J. Phys. Chem. B* **2007**, *111*, 4877−4884. (d) Liu, L.; Li, S.; Cao, Z.; Peng, Y.; Li, G.; Yan, T.; Gao, X.-P. *J. Phys. Chem. B* **2007**, *111*, 12161−12164. (e) Kornyshev, A. A. *J. Phys. Chem. B* **2007**, *111*, 5545−5557.

(17) (a) Daguenet, C.; Dyson, P. J.; Krossing, I.; Oleinikova, A.; Slattery, J.; Wakai, C.; Weingärtner, H. *J. Phys. Chem. B* **2006**, *110*, 12682−12688. (b) Halder, M.; Headley, S.; Mukherjee, P.; Song, X.; Petrich, J. W. *J. Phys. Chem. B* **2006**, *110*, 8623−8626. (c) Ito, N.; Richert, R. *J. Phys. Chem. B* **2007**, *111*, 5016−5022.

(18) Zusman, L. D. *Electrochim. Acta* **1991**, *36*, 395−399.

(19) Marcus, R. A. *J. Phys. Chem. B* **1998**, *102*, 10071−10077.

(20) Buttry, D. A.; Anson, F. C. *J. Am. Chem. Soc*. **1983**, *105*, 685−689.

(21) (a) Harper, A. S.; Leone, A. M.; Lee, D.; Wang, W.; Ranganathan, S.; Williams, M. E.; Murray, R. W. *J. Phys. Chem. B* **2005**, *109*, 18852−18859. (b) Ranganathan, S.; Murray, R. W. *J. Phys. Chem. B* **2004**, *108*, 19982−19989. (c) Wang, W.; Lee, D.; Leone, A. M.; Murray, R. W. *Chem. Phys.* **2005**, *319*, 126−135.

(22) (a) Illner, P.; Zahl, A.; Puchta, R.; van Eikema Hommes, N.; Wasserscheid, P.; van Eldik, R. *J. Organomet. Chem*. **2005**, *690*, 3567−3576. (b) Bonhote, P.; Dias, A.; Papageorgiou, N.; Kalyanasundaram, K.; Gratzel, M. *Inorg. Chem.* **1996**, *35*, 1168−1178. (c) Skrzypczak, A.; Neta, P. *J. Phys. Chem. A* **2003**, *107*, 7800−7803. (d) Evans, G. R.; Compton, R. G. *ChemPhysChem* **2006**, *7*, 488−496.

(23) Mahlendorf, F.; Heinze, J. *J. Electroanal. Chem*. **1993**, *352*, 119−130.

(24) (a) Nicholson, R. S. *Anal. Chem*. **1965**, *37*, 1351−1355. (b) Nicholson, R. S.; Shain, I. *Anal. Chem*. **1964**, *36*, 706−723.

(25) (a) Compton, R. G. University of Oxford, Oxford, U.K. Private communication, 2007 (and ref 22d). (b) Schmitz, J. E. J.; van der Lindeen, J. G. M. *Anal. Chem*. **1982**, *54*, 1879−1880.

(26) (a) Rooney, M. B.; Coomber, D. C.; Bond, A. M. *Anal. Chem*. **2000**, *72*, 3486−3491. (b) Bond, A. M.; Feldberg, S. W. *J. Phys. Chem. B* **1998**, *102*, 9966−9974.

(27) (a) Bond, A. M.; Oldham, K .B.; Snook, G. A. *Anal. Chem*. **2000**, *72*, 3492−3496. (b) Oelssner, W.; Berthold, F.; Guth, U. *Mater. Corros.* **2006**, *57*, 455−466.

(28) (a) Först, P.; Werner, F.; Delgado, A. *Rheol. Acta* **2000**, *39*, 566−573. (b) Först, P.; Werner, F.; Delgado, A. *Rheol. Acta* **2002**, *41*, 369−374. (c) Schopper, A.; Predel, T.; Schlücker, E. Bachelor Thesis, University of Erlangen-Nürnberg, 2006.

(29) (a) Bockris, J. O'M.; Hooper, G. W. *Discuss. Faraday. Soc*. **1962**, *32*, 218−236. (b) Noda, A.; Hayamizu, K.; Watanabe, M. *J. Phys. Chem. B* **2001**, *105*, 4603−4610. (c) Xu, W.; Cooper, E. I.; Angell, C. A. *J. Phys. Chem. B* **2003**, *107*, 6170−6178.

(30) Nadler, W.; Marcus, R. A. *Chem. Phys. Lett.* **1988**, *144*, 24−30.

(31) Okoturo, O. O.; van der Noot, T. J. *J. Electroanal. Chem*. **2004**, *568*, 167−181.

(32) (a) Marcus, R. A.; Sutin, N. *Biochim. Biophys. Acta* **1985**, *811*, 265−322. (b) Brunschwig, B. S.; Sutin, N. *Coord. Chem. Rev.* **1999**, *187*, 233−254.

(33) Fawcett, W. R.; Blum, L. *Chem. Phys. Lett*. **1991**, *187*, 173−179.

(34) (a) Becka, A. M.; Miller, C. J. *J. Phys. Chem.* **1992**, 96, 2657−2668. (b) Terrettaz, A.; Becka, A. M.; Traub, M. J.; Fettinger, J. C.; Miller, C. J. *J. Phys. Chem.* **1995**, *99*, 11216−11224.

(35) Liu, Y. P.; Newton, M. D. *J. Phys. Chem*. **1994**, *98*, 7162−7170.

(36) (a) Dolidze, T. D.; Agladze, T. R. *Bull. Georgian Acad. Sci.* **1990**, *139*, 317−320. (b) Mareček, V.; Samec, Z.; Weber, J. *J. Electroanal. Chem.* **1978**, *94*, 169−185.

(37) (a) McManis, G. E.; Nielson, R. M.; Gochev, A.; Weaver, M. J. *J. Am. Chem. Soc.* **1989**, *111*, 5533−5541. (b) Fawcett, W. R.; Foss, C. A. *Electrochim. Acta* **1991**, *36*, 1767−1774.

(38) Gosavi, S.; Marcus, R. A. *J. Phys. Chem. B* **2000**, *104*, 2067−2072.

(39) (a) Gavish, B.; Yedgar, S. In *Protein−Solvent Interactions*; Gregory, R.B., Ed.; Marcel Dekker: New York, 1995; pp 343−373. (b) Fenimore, P. W.; Frauenfelder, H.; McMahon, B. H.; Parak, F. G. *Proc. Natl. Acad. Sci. U.S.A.* **2002**, *99*, 16047−16051.

(40) (a) Karmakar, R.; Samanta, A. *J. Phys. Chem. A* **2003**, *107*, 7340−7346. (b) Ingram, J. A.; Moog, R. S.; Biswas, N. I. R.; Maroncelli, M. *J. Phys. Chem. B* **2003**, *107*, 5926−5932. (c) Shirota, H.; Castner, E. W. *J. Phys. Chem. A* **2005**, *109*, 9388−9392. (d) Hu, Z.; Margulis, J. C. *J. Phys. Chem. B* **2006**, *110*, 11025−11028. (e) Arzhantsev, S.; Jin, H.; Ito, N.; Maroncelli, M. *Chem. Phys. Lett*. **2006**, *417*, 524−529.

(41) Hu, Z.; Margulis, J. C. *Proc. Natl. Acad. Sci. U.S.A.* **2006**, *103*, 831−836.

(42) (a) Adam, G.; Gibbs, J. W. *J. Chem. Phys.* **1965**, *43*, 139−146. (b) Angell, C. A.; Ngai, K. L.; McMillan, P. F.; Martin, S. W. *Appl. Phys. Rev.* **2000**, *88*, 3113−3157. (c) Johari, G. P. *J. Chem. Phys.* **2000**, *112*, 8958−8969. (d) Stevenson, J. D.; Schmalian, J.; Wolynes, P. G. *Nat. Phys.* **2006**, *2*, 268−274.

(43) (a) Sachinidis, J. I.; Shalders, R. D.; Tregloan, P. A. *Inorg. Chem.* **1996**, *35*, 2497−2503. (b) Swaddle, T. W.; Tregloan, P. A. *Coord. Chem. Rev.* **1999**, *187*, 255−289. (c) Sachinidis, J. I.; Shalders, R. D.; Tregloan, P. A. *Inorg. Chem.* **1994**, *33*, 6180−6186.

(44) (a) Hupp, J. T.; Weaver, M. J. *Inorg. Chem.* **1984**, *23*, 3639−3644. (b) Hupp, J. T.; Weaver, M. J. *Inorg. Chem.* **1984**, *23*, 256−258.

(45) Tran, D.; Hunt, J. P.; Wherland, S. *Inorg. Chem.* **1992**, *31*, 2460−2464.